Satellite Image Atlas
of Glaciers of the World

IRIAN JAYA, INDONESIA,
and
NEW ZEALAND

United States Geological Survey
Professional Paper 1386–H

Cover: Oblique aerial photograph of the Garden of Eden and Garden of Allah ice fields in the Southern Alps, New Zealand. See page H28.

GLACIERS OF IRIAN JAYA, INDONESIA, AND NEW ZEALAND—

H–1. GLACIERS OF IRIAN JAYA, INDONESIA
By IAN ALLISON *and* JAMES A. PETERSON

H–2. GLACIERS OF NEW ZEALAND
By TREVOR J.H. CHINN

SATELLITE IMAGE ATLAS OF GLACIERS OF THE WORLD

Edited by RICHARD S. WILLIAMS, Jr., *and* JANE G. FERRIGNO

U. S. GEOLOGICAL SURVEY PROFESSIONAL PAPER 1386–H

UNITED STATES GOVERNMENT PRINTING OFFICE, WASHINGTON: 1989

U.S. DEPARTMENT OF THE INTERIOR

BRUCE BABBITT, ***Secretary***

U.S. GEOLOGICAL SURVEY

Gordon P. Eaton, ***Director***

Reprinted 1995

Library of Congress Cataloging in Publication Data
(Revised for vol. 2)

Satellite image atlas of glaciers of the world.

(U.S. Geological Survey professional paper ; 1386)
Two fold. col. maps in pocket in v. B.
Includes bibliographical references.
Supt. of Docs. no.: I 19.16:1386–H
Contents: —ch. B. Antarctica / by Charles Swithinbank ; with sections on The "dry valleys" of Victoria Land, by Trevor J.H. Chinn, [and] Landsat images of Antarctica, by Richard S. Williams, Jr., and Jane G. Ferrigno—ch. H, 1. Glaciers of Irian Jaya, Indonesia / by Ian Allison and James A. Peterson—ch. H, 2. Glaciers of New Zealand / by Trevor J.H. Chinn
GB2401.72.R42S28 1988 551.3′12 87–600497

For sale by the U.S. Geological Survey, Information Services
Box 25286, Federal Center, Denver, CO 80225

Foreword

On 23 July 1972, the first Earth Resources Technology Satellite (ERTS 1 or Landsat 1) was successfully placed in orbit. The success of Landsat inaugurated a new era in satisfying mankind's desire to better understand the dynamic world upon which we live. Space-based observations have now become an essential means for monitoring global change.

The short- or long-term cumulative effects of processes that cause significant changes on the Earth's surface can be documented and studied by repetitive Landsat images. Such images provide a permanent historical record of the surface of our planet; they also make possible comparative two-dimensional measurements of change over time. This Professional Paper demonstrates the importance of the application of Landsat images to global studies by using them to determine the current distribution of glaciers on our planet. As images become available from future satellites, the new data will be used to document global changes in glacier extent by reference to the image record of the 1970's.

Although many geological processes take centuries or even millenia to produce obvious changes on the Earth's surface, other geological phenomena, such as glaciers and volcanoes, cause noticeable changes over shorter periods. Some of these phenomena can have a worldwide impact and often are interrelated. Explosive volcanic eruptions can produce dramatic effects on the global climate. Natural or culturally induced processes can cause global climatic cooling or warming. Glaciers respond to such warming or cooling periods by decreasing or increasing in size, thereby causing sea level to rise or fall.

As our understanding of the interrelationship of global processes improves and our ability to assess changes caused by these processes develops further, we will learn how to use indicators of global change, such as glacier variation, to more wisely manage the use of our finite land and water resources. This Professional Paper is an excellent example of the way in which we can use technology to provide needed earth-science information about our planet. The international collaboration represented by this report is also an excellent model for the kind of cooperation that scientists will increasingly find necessary in the future in order to solve important earth-science problems on a global basis.

Dallas L. Peck
Director,
U.S. Geological Survey

Preface

This chapter is 1 in a series of 11 that comprise U.S. Geological Survey Professional Paper 1386, Satellite Image Atlas of Glaciers of the World, which is directed at the use of remotely sensed images, primarily from the Landsat 1, 2, and 3 series of spacecraft, to document, monitor, and study the glacierized regions of our planet. Although Landsat 1, 2, and 3 multispectral scanner (MSS) and Landsat 3 return beam vidicon (RBV) images are especially well suited to studying changes in the Antarctic ice sheet (Chapter B), the Greenland ice sheet (Chapter C), and ice caps and (or) ice fields in Iceland (Chapter D), Europe (Chapter E), Asia (Chapter F), South America (Chapter I), and North America (Chapter J), the images can also be used, in conjunction with maps, aerial photographs, and field measurements, to study and monitor changes in smaller glaciers on high mountains at lower latitudes, if the glaciers reach a size of a few kilometers (length or diameter).

In Irian Jaya, Indonesia, three small perennial ice fields are located on Puncak Jaya massif, Puncak Mandala, and Ngga Pilimsit in the Central Range. The largest ice field, on Puncak Jaya massif, has an area of approximately 7 km^2. All three ice fields have experienced rapid retreat during the 20th century, a situation that has been documented at other equatorial glaciers in Africa (Chapter G) and South America (Chapter I). Landsat images were combined with field observations to locate, delineate, and monitor changes in the ice field.

In New Zealand, approximately 3,155 glaciers occur along the crest of the Southern Alps, South Island, and 6 glaciers are present on Mount Ruapehu, North Island. The total area covered is about 1,159 km^2, with an estimated volume of 53.3 km^3. In 1859, the first observations were made of New Zealand's glaciers; in 1889, the first precise measurements were carried out, although modern glaciological studies were not begun until the 1950's. Because of limitations in spatial resolution of the sensors, Landsat images were found to be useful only for monitoring changes in the largest glaciers and in the position of the transient snowline.

Richard S. Williams, Jr.
Jane G. Ferrigno,
Editors

About this Volume

U.S. Geological Survey Professional Paper 1386, Satellite Image Atlas of Glaciers of the World, contains eleven chapters designated by the letters A through K. Chapter A is a general chapter containing introductory material and a discussion of the physical characteristics, classification, and global distribution of glaciers. The next nine chapters, B through J, are arranged geographically and present glaciological information from Landsat and other sources of data on each of the geographic areas. Chapter B covers Antarctica; Chapter C, Greenland; Chapter D, Iceland; Chapter E, Continental Europe (except for the European part of the Soviet Union), including the Alps, the Pyrenees, Norway, Sweden, Svalbard (Norway), and Jan Mayen (Norway); Chapter F, Asia, including the European part of the Soviet Union, China (P.R.C.), India, Nepal, Afghanistan, and Pakistan; Chapter G, Turkey, Iran, and Africa; Chapter H, Irian Jaya (Indonesia) and New Zealand; Chapter I, South America; and Chapter J, North America. The final chapter, K, is a topically oriented chapter that presents related glaciological topics.

The realization that one element of the Earth's cryosphere, its glaciers, was amenable to global inventorying and monitoring with Landsat images led to the decision, in late 1979, to prepare this Professional Paper, in which Landsat 1, 2, and 3 multispectral scanner (MSS) and Landsat 2 and 3 return beam vidicon (RBV) images would be used to inventory the areal occurrence of glacier ice on our planet within the boundaries of the spacecraft's coverage (between about 81° north and south latitudes). Through identification and analysis of optimum Landsat images of the glacierized areas of the Earth during the first decade of the Landsat era, a global benchmark could be established for determining the areal extent of glaciers during a relatively narrow time interval (1972 to 1982). This global "snapshot" of glacier extent could then be used for comparative analysis with previously published maps and aerial photographs and with new maps, satellite images, and aerial photographs to determine the areal fluctuation of glaciers in response to natural or culturally induced changes in the Earth's climate.

To accomplish this objective, the editors selected optimum Landsat images of each of the glacierized regions of our planet from the Landsat image data base at the EROS Data Center in Sioux Falls, South Dakota, although some images were also obtained from the Landsat image archives maintained by the Canada Centre for Remote Sensing, Ottawa, Ontario, Canada, and by the European Space Agency in Kiruna, Sweden, and Fucino, Italy. Between 1979 and 1981, these optimum images were distributed to an international team of more than 50 scientists who agreed to author a section of the Professional Paper concerning either a geographic area or a glaciological topic. In addition to analyzing images of a specific geographic area, each author was also asked to summarize up-to-date information about the glaciers within the area and to compare their present areal distribution with historical information (for example, from published maps, reports, photographs, etc.) about their past extent. Completion of this atlas will provide an accurate regional inventory of the areal extent of glaciers on our planet during the 1970's.

Richard S. Williams, Jr.
Jane G. Ferrigno,
Editors

CONTENTS

Glaciers of Irian Jaya, Indonesia, and New Zealand—

GLACIERS OF IRIAN JAYA, INDONESIA

By IAN ALLISON *and* JAMES A. PETERSON

SATELLITE IMAGE ATLAS OF GLACIERS OF THE WORLD

Edited by RICHARD S. WILLIAMS, Jr., *and* JANE G. FERRIGNO

U. S. GEOLOGICAL SURVEY PROFESSIONAL PAPER 1386–H–1

Landsat images, in conjunction with aerial photographs and field measurements, were used to locate, describe, and monitor changes in the three ice fields in the Central Range of Irian Jaya

UNITED STATES GOVERNMENT PRINTING OFFICE, WASHINGTON : 1989

CONTENTS

GLACIERS OF IRIAN JAYA, INDONESIA, AND NEW ZEALAND—

GLACIERS OF IRIAN JAYA, INDONESIA

By IAN ALLISON[1] *and* JAMES A. PETERSON[2]

Abstract

Three small perennial ice fields with a total area of about 7.5 ± 0.5 km^2 are situated on Puncak Jaya massif, Puncak Mandala, and Ngga Pilimsit in the Central Range of Irian Jaya. The largest of these is the one on Puncak Jaya massif with an area of about 7 km^2. The other ice fields each have a diameter of only several hundred meters. All the ice fields have experienced extensive and rapid retreat during this century. Landsat imagery has been used in conjunction with field measurements to locate, describe, and monitor changes in the ice fields.

Introduction

The high peaks of the 2,500-km-long Pegunungan Maoke [3] or Central Range, of equatorial New Guinea presently support glaciers in three ice areas, all of which are in the Indonesian territory of Irian Jaya: the Puncak Jaya massif (Carstensz; 4°05'S., 137°11'E.; 4,884 m), Puncak Mandala (Julianatop; 4°48'S., 140°20'E.; 4,640 m), and Ngga Pilimsit (Idenburg-top; 4°03'S., 137°02'E.; 4,717 m) (fig. 1). An ice cap on Puncak Trikora (Wilhelmina-top; 4°15'S., 138°45'E.; 4,730 m) disappeared sometime between 1939 and 1962. The extensive retreat of all these glaciers, which has occurred during this century, has been documented by Mercer (1967) and by Peterson and others (1973).

The largest of these ice-covered areas, on the massif dominated by Puncak Jaya, totals about 7 km^2. This area was studied in some detail by two Australian Universities' Carstensz Glaciers Expeditions (CGE), and the ice area and their recent history of retreat are described by Allison and Peterson (1976). The glaciers are situated atop a ridge of folded Tertiary limestone, the axis of which trends west-northwest to east-southeast, and can be divided into four main ice masses (fig. 2): the Northwall Firn (separated into three parts by 1972), the Meren Glacier, the Carstensz Glacier (plus the small niche glaciers, the Wollaston and

[1]Australian Antarctic Division, Channel Highway, Kingston, Tasmania 7050, Australia.
[2]Department of Geography, Monash University, Wellington Road, Clayton, Victoria 3168, Australia.
[3]The names used are those approved by the U.S. Board of Geographic Names and published by Garren and others (1982). In the case of glaciers and other geographic features where there is no officially approved name, the name generally accepted in the glaciological literature has been used.

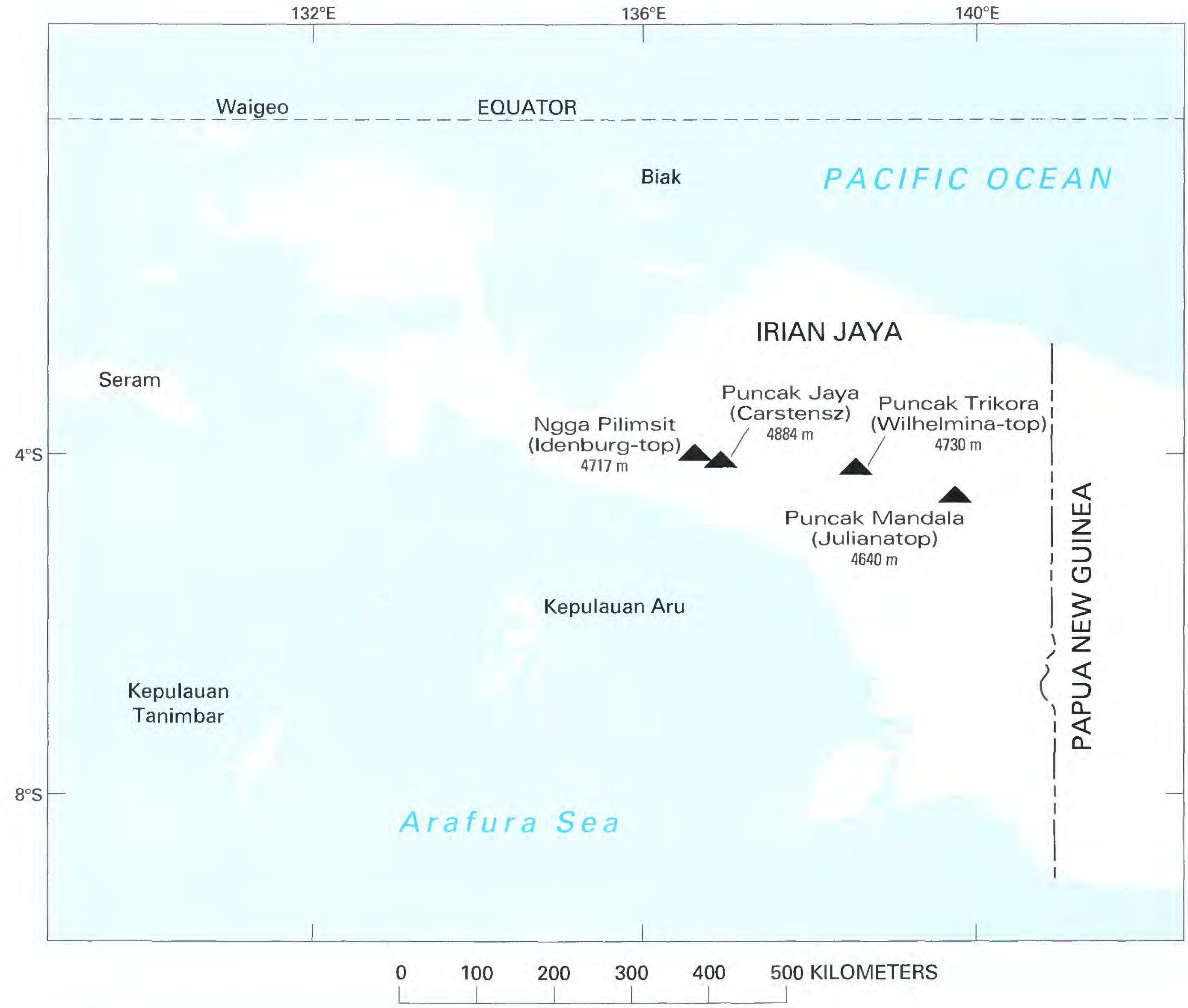

Figure 1.*—Index map of Irian Jaya showing the location of the highest mountains (after fig. 1 in Peterson and others, 1973).*

Van de Water, which descend from the same firn field), and the Southwall Hanging Glaciers. Details of these ice masses are tabulated by Müller (1977).

The Meren and Carstensz Glaciers flow westward in parallel glacial valleys, the Meren Valley and Yellow Valley, respectively (figs. 2, 3). In 1972, the Meren Glacier had an area of 1.9 km^2, a mean thickness of 40 m, and measured surface velocities of up to 30 m a^{-1}; the Carstensz Glacier had an area of 0.9 km^2, a mean thickness of 38 m, and measured surface velocities of up to 18 m a^{-1}. The morphology and dynamics of both these glaciers are described by Allison (1975 and 1976).

Seasonal climatic variations on the Puncak Jaya massif are very slight. Monthly mean temperatures vary by less than 0.5 °C during the year, and there appears to be no marked seasonal variation in precipitation, radiation, or cloud cover (Allison and Bennett, 1976). As a consequence, the net balance of the glaciers remains seasonally uniform, and ablation occurs year round below the equilibrium line; above the equilibrium line accumulation occurs year round. Hence the snowline elevation on the glacier remains near the equilibrium-line altitude except for short periods after heavy snowfalls. Mass-balance measurements in 1972 indicated an equilibrium-line altitude of 4,580 m with the net annual balance reaching +1 m a^{-1} water equivalent (w.e.) at 4,800 m elevation, near the top of the glaciers, and −5 m a^{-1} w.e. at 4,400 m, near the termini. Because ablation occurs throughout the year in the ablation zone, the vertical budget gradient (activity index) for these glaciers is high. Both the Meren and Carstensz Glaciers had a negative mass budget in 1972, which is consistent with their observed retreat.

The ice extent on the Puncak Jaya massif is small, but the area is one of only a few present-day, ice-covered equatorial regions. The rapid and continuing retreat of the glaciers during this century indicates that the mass budget has been consistently negative. This suggests a climatic change, of which the glaciers are a sensitive indicator. Using a numerical model of the glaciers and their dynamics, Allison and Kruss (1977) estimated the change in mass budget necessary to give the observed retreat, between about 1850 and 1972, of more than 2 km for the Carstensz and more than 3 km for the Meren Glacier. They showed that a steady rise of the equilibrium-line elevation at a rate of 80 m per century allowed the model to match the observed retreat and that the most likely explanation for the mass-balance change was a warming of the regional air temperature by 0.6 °C per century.

Subsequent observations show that the terminus of the Meren Glacier retreated about 200 m between 1973 and 1976 and that the Carstensz Glacier retreated 50 m during the same period of time (Dr. L. Hansen, pers. commun.). Continued monitoring of the glaciers is obviously needed because of the climatic implications.

Far less, however, is known about the other glaciers in Irian Jaya. The ice caps on Ngga Pilimsit (about 12 km northwest of Puncak Jaya) and on Puncak Mandala each have a diameter of only several hundred meters (Mercer, 1967; Peterson and others, 1973).

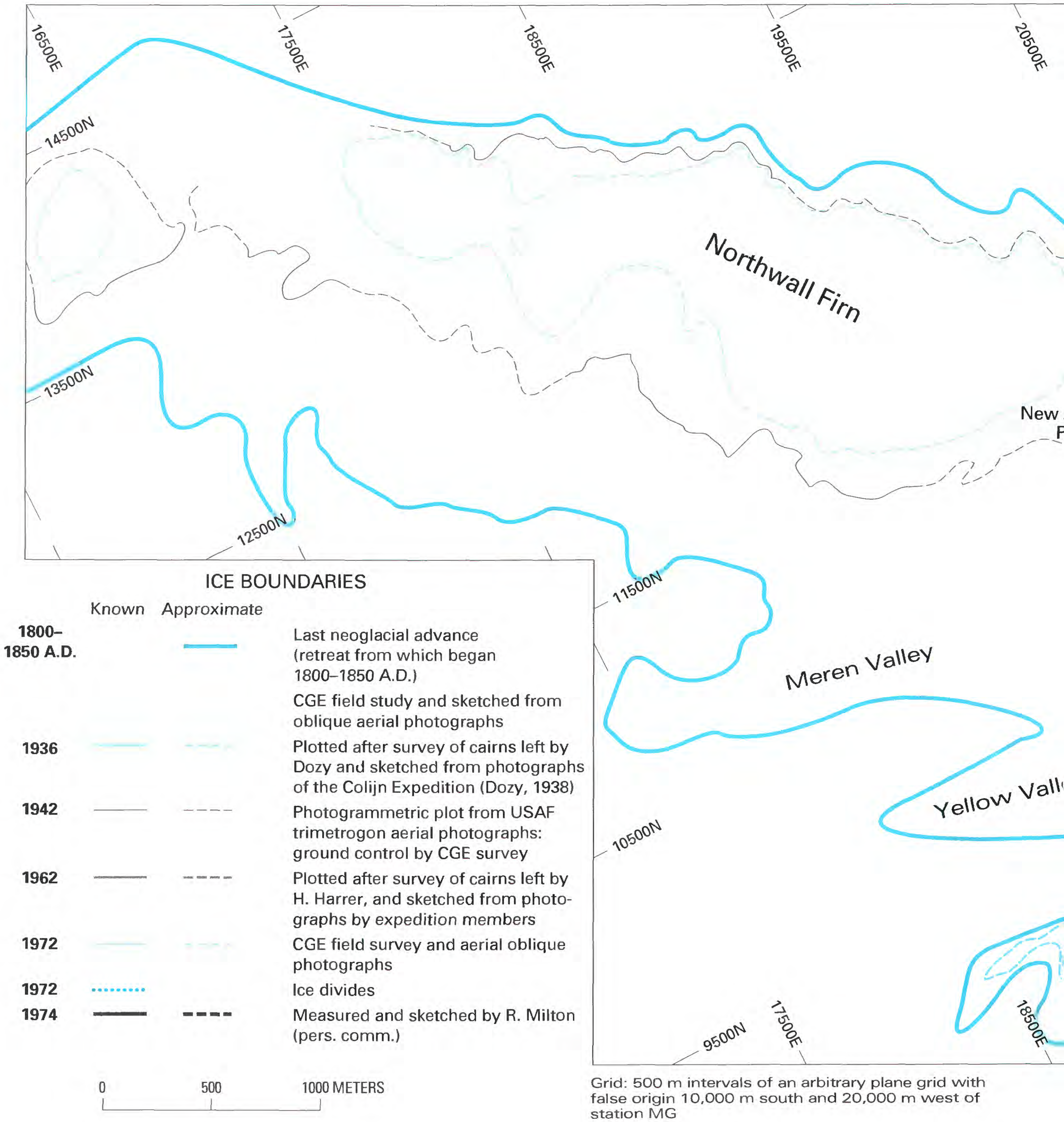
16500E
17500E
18500E
19500E
20500E
14500N
13500N
12500N
11500N
10500N
9500N
17500E
18500E
Northwall Firn
New
Meren Valley
Yellow Vall
ICE BOUNDARIES
Known
Approximate
1800–1850 A.D.
Last neoglacial advance (retreat from which began 1800–1850 A.D.)
CGE field study and sketched from oblique aerial photographs
1936
Plotted after survey of cairns left by Dozy and sketched from photographs of the Colijn Expedition (Dozy, 1938)
1942
Photogrammetric plot from USAF trimetrogon aerial photographs: ground control by CGE survey
1962
Plotted after survey of cairns left by H. Harrer, and sketched from photographs by expedition members
1972
CGE field survey and aerial oblique photographs
1972
Ice divides
1974
Measured and sketched by R. Milton (pers. comm.)
0
500
1000 METERS
Grid: 500 m intervals of an arbitrary plane grid with false origin 10,000 m south and 20,000 m west of station MG

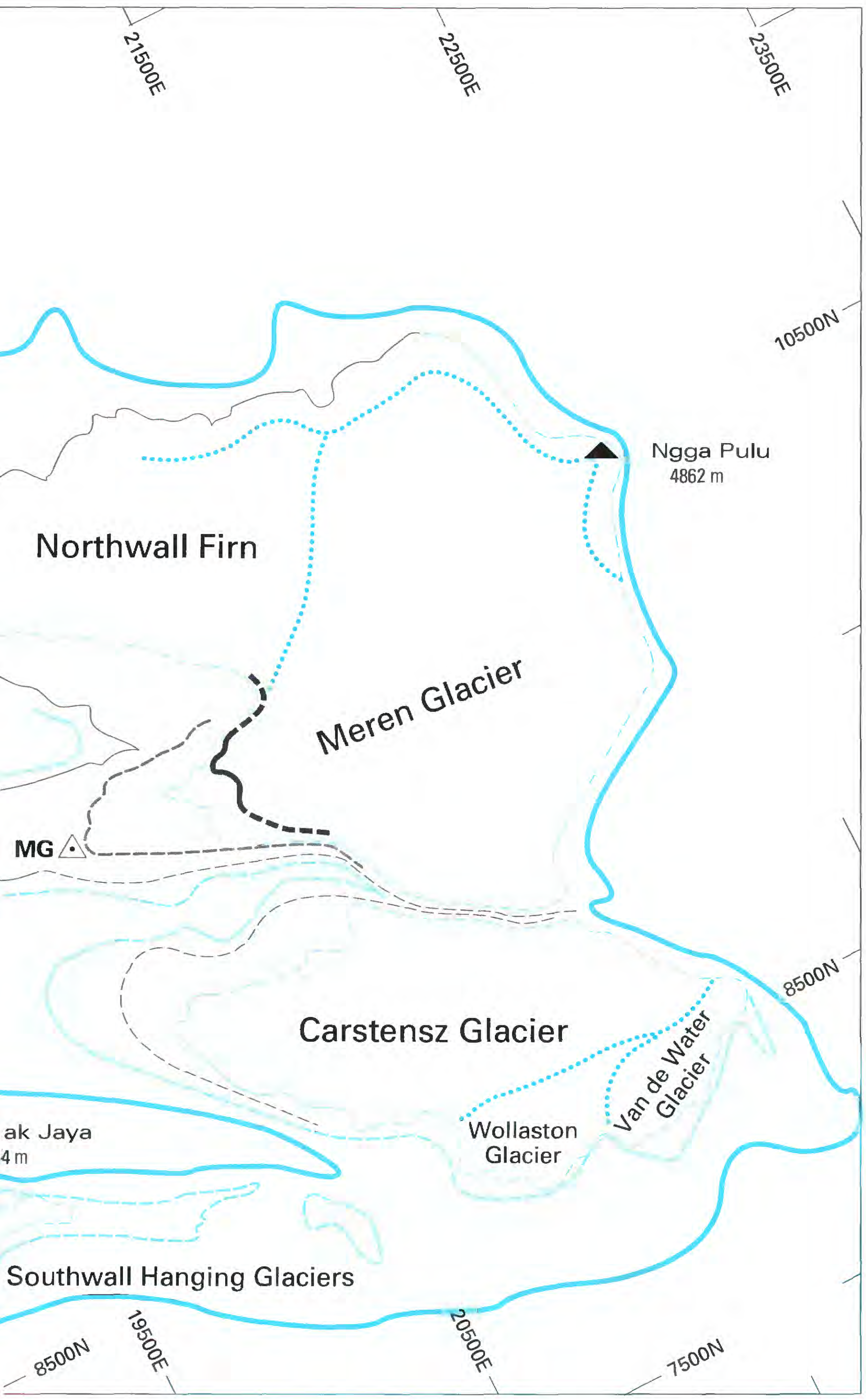

***Figure 2.**—Map of the ice fields of the Puncak Jaya area showing retreat of the ice boundaries since about 1800 to 1850 A.D. (from 1:20,000-scale Australian Universities' Carstensz Glaciers Expeditions).*

Figure 3.—*Oblique aerial photograph looking east at several of the glaciers on Puncak Jaya in 1936. Left to right: North-wall Firn, Meren Glacier, and Carstensz Glacier. Photograph no. S.136 by J.J. Dozy.*

Glacier Imagery and Mapping

Aerial Photography

Because of the area's remoteness and the persistent cloud cover, the available aerial photography of the Irian Jaya glaciers is limited. Before 1975, the only vertical aerial photographs of the Puncak Jaya glaciers were obtained in 1942 during an aerial survey, with a trimetrogon camera, by the United States Army Air Force (USAAF). Most of the Northwall Firn is covered in three vertical frames acquired along one flight line of this survey (USAAF photograph no. 4 CS-5MC20-23V, frames 117 to 119, fig. 4), but the two major valley glaciers (the Meren and the Carstensz), the western end of the Northwall Firn, and Ngga Pilimsit are covered only by the trimetrogon oblique aerial photographs (USAAF photograph nos. 23R-119 (fig. 5), 23L-117, and 23L-113, respectively). The ice fields on the south wall are not covered by this flight line.

More recent medium altitude (up to 11,500 m), vertical aerial photographs of the region were obtained during combined Indonesian and Australian military mapping operations between 1976 and 1981. Photographs V2F-RAAF-8466, Run 19E, frames 190-194, September 1976, cover the Northwall Firn only, while photographs V2F-RAAF-9922, Run 0022, frames 9147 and 9148, January 1981, give complete coverage of the glaciers on the massif but were taken after a snowfall, which makes determination of the ice margins difficult.

Data on the reduction of the total glaciated area on the Puncak Jaya massif come mostly from oblique aerial photographs. These include those taken during the 1936 Colijn Expedition (Dozy, 1938; Mercer, 1967) (see fig. 3), during the 1971/72 CGE (fig. 6), and during occasional light aircraft overflights of the area. The rapid retreat of the Puncak Jaya glaciers is shown dramatically by comparing figure 3 with figure 6.

Reports of changes of the ice caps on Ngga Pilimsit and Puncak Mandala have been based on oblique aerial photography and some ground-based observations (Mercer, 1967; Peterson and others, 1973).

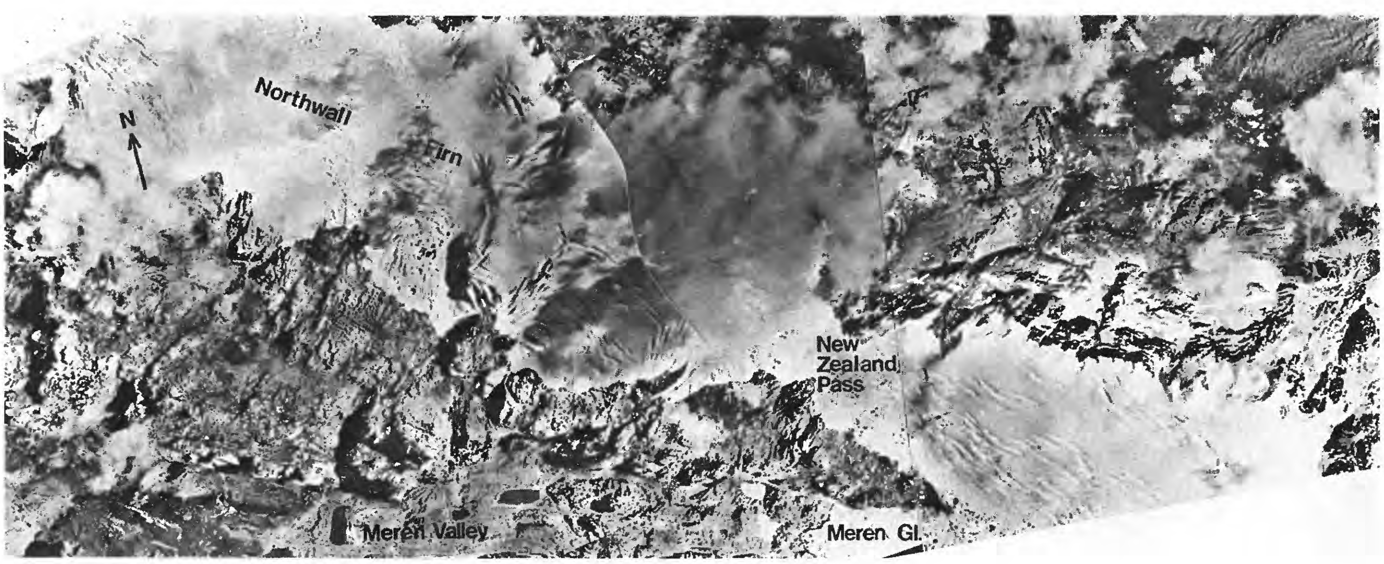

***Figure 4.**—Mosaic of U.S. Army Air Force vertical aerial photographs of the Northwall Firn in 1942.*

Figure 5.—*U.S. Army Air Force trimetrogon oblique aerial photograph looking south at the glaciers in 1942. Foreground, Northwall Firn; center, Meren Glacier; background, Carstensz Glacier.*

Figure 6.—*Oblique aerial photograph looking east at the glaciers in 1972. Photograph acquired during the Carstensz Glaciers Expeditions (CGE). Compare with figure 3. Left to right: Northwall Firn, Meren Glacier, and Carstensz Glacier.*

Maps of the Puncak Jaya Region and of the Glacier Recession

The largest-scale map of the Puncak Jaya glacier area is a 1:20,000-scale topographic map, produced by the CGE from the 1971 to 1973 ground survey and photogrammetry of the 1942 USAAF vertical aerial photographs (using CGE ground control) (Anderson, 1976). The contour interval over most of this map is 50 m, with a 10-m contour interval on the Carstensz and Meren Glaciers.

The ice limits at different times, as shown in figure 2, are based on this map. The reliability of the ice limits is indicated in the explanation. While the reliability is generally good at the snouts of the Meren and Carstensz Glaciers, the eastern and southern ice boundaries are based only on uncontrolled oblique aerial photographs.

A small-scale map (1:250,000) was used by the CGE to delineate the maximum extent of the last Pleistocene (Wisconsinan, or Würm) glaciation. This map was based on the 1:250,000-scale Joint Operations Graphic Series 1501, Sheets SB53–4 and SB53–16, with corrections made to the drainage net from field observations. The glacial geology features (morainal ridges, glaciated headwalls, and probable maximum extent of glaciation) were mapped from the 1942 USAAF trimetrogon oblique aerial photographs and field reconnaissance by the CGE and others (Hope and Peterson, 1976).

Satellite Imagery

The inaccessibility of the region for both conventional and aerial surveys makes monitoring of the glaciers by satellite a particularly attractive proposition. Because the largest of the glaciers on Puncak Jaya covers less than 7 km^2, only the Landsat series of spacecraft has offered sufficient resolution for mapping even gross changes. Unfortunately, the mountains of New Guinea are usually obscured by cloud cover, and only one Landsat image (see fig. 8) showing the Puncak Jaya glaciers prior to 1980 is available (1643–00253, band 7; 27 April 1974; Path 110, Row 63) (fig. 7 and table 1).

More recent images showing the glaciers have, however, become available since the Australian Landsat station started to receive data from the Irian Jaya region in 1980. The Puncak Jaya and Ngga Pilimsit glaciers are clearly seen in Landsat 4 multispectral scanner (MSS) images for 8 September 1982, 30 January 1983, and 19 March 1983, while the small Puncak Mandala ice cap can be identified in a Landsat 2 MSS image for 19 August 1981 and Landsat 4 MSS images for 21 March 1983 and 3 January 1984 (table 1).

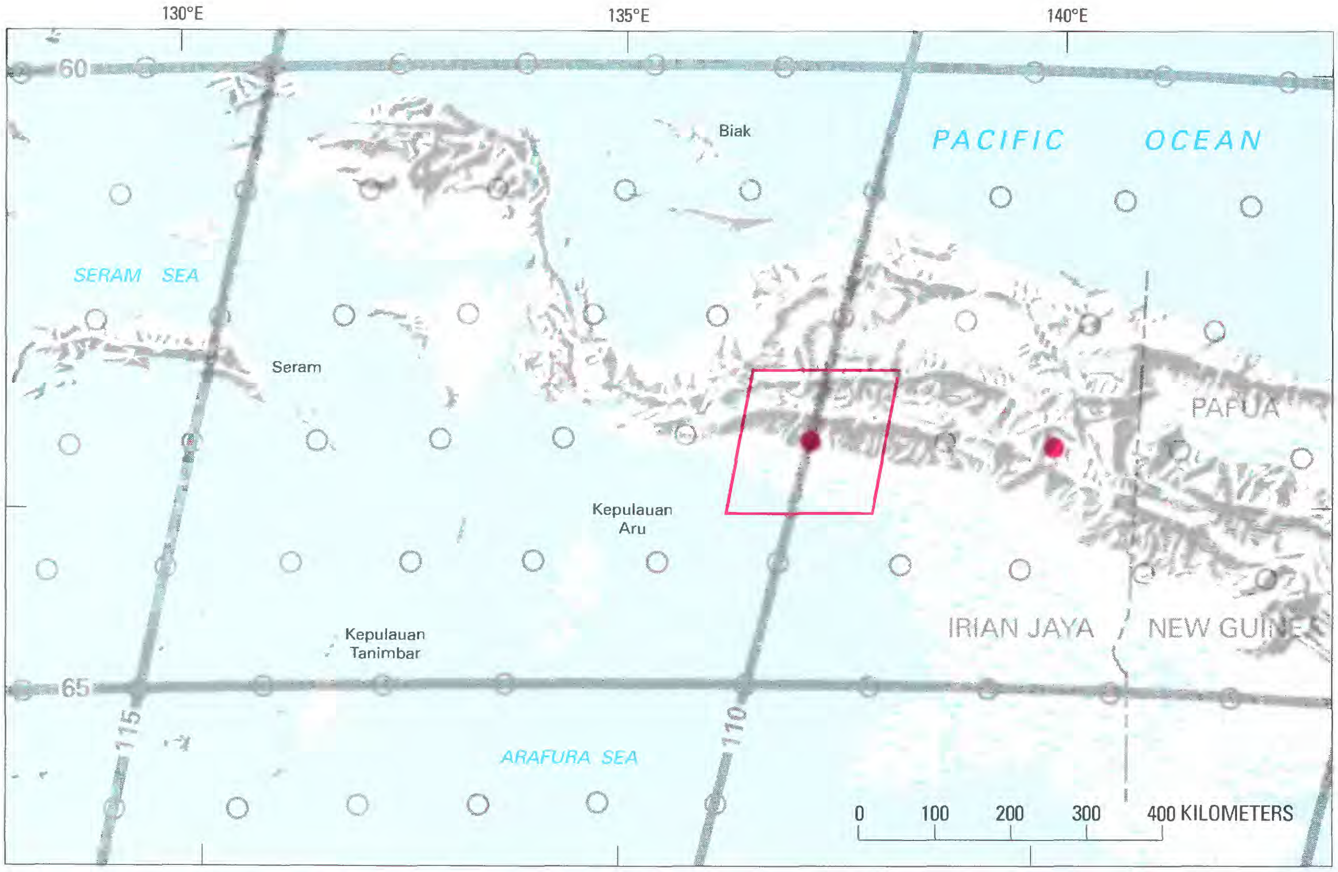

EXPLANATION OF SYMBOLS

Evaluation of image usability for glaciologic, geologic, and cartographic applications. Symbols defined as follows:

- ● Excellent image (0 to ≤5 percent cloud cover)
- ○ Nominal scene center for a Landsat image outside the area of glaciers
- ▱ Approximate size of area encompassed by nominal Landsat MSS image

Figure 7.*—Index map to the optimum Landsat 1, 2, and 3 images of the glaciers of Irian Jaya.*

TABLE 1.—*Optimum Landsat 1, 2, and 3 images of the glaciers of Irian Jaya*

[Five optimum Landsat 4 MSS images are also included in the table to provide better coverage of the glacierized areas of Irian Jaya. These images were found by the authors, but it is possible that better, more recent imagery of the area is available. In the "Code" column, a filled-in circle means an excellent image (0 to ≤5 percent cloud cover); a filled semicircle means a fair to poor image (>10 to≤ 100 percent cloud cover)]

Path-Row	Nominal scene center (lat.-long.)	Landsat identification number	Date	Solar elevation angle (in degrees)	Code	Cloud cover (in percent)	Remarks
				Landsat 1–3			
108–63	004° 20′S. 140° 03′E.	22113–00073	04 Nov 80	51	◐	60	Covers Puncak Mandala glacier area, but cloud in immediate glacier region; color composite available; archived by Australian Landsat Station
108–63	004° 20′S. 140° 03′E.	22401–00035	19 Aug 81	48	●	0	As above but largely cloud free around glacier; color composite available; archived by Australian Landsat Station
110–63	004° 20′S. 137° 11′E.	1643–00253	27 Apr 74	50	●	0	Covers Puncak Jaya and Ngga Pilimsit glacier areas; color composite available
110–63	004° 20′S. 137° 11′E.	30716–00153	19 Feb 80	51	◐	90	As above; mostly high, thin cloud except along the main range; glacier partly obscured; color composite and partial scenes available; archived by Australian Landsat Station
				Landsat 4			
101–63	004° 20′S. 139° 58′E.	40248–00191	21 Mar 83	55	◐	50	Covers Puncak Mandala glacier area; glacier region partly cloud free; archived by Australian Landsat Station
101–63	004° 20′S. 139° 58′E.	40536–00182	03 Jan 84	51	◐	80	As above but more cloud in glacier region; archived by Australian Landsat Station
103–63	004° 20′S. 136° 53′E.	40054–00292	08 Sep 82	53	●	0	Covers Puncak Jaya and Ngga Pilimsit regions; glaciers cloud free; archived by Australian Landsat Station
103–63	004° 20′S. 136° 53′E.	40198–00313	30 Jan 83	53	◐	50	Covers Puncak Jaya and Ngga Pilimsit; scattered cloud in glacier region; archived by Australian Landsat Station
103–63	004° 20′S. 136° 53′E.	40246–00313	19 Mar 83	54	◐	20	As above but less cloud in glacier region (only on the southern side of main range); archived by Australian Landsat Station

Observation and Mapping of the Glaciers Shown on Landsat Images

Puncak Jaya and Ngga Pilimsit

The Landsat scene (1643–00253, band 7; 27 April 1974; Path 110, Row 63), which includes the Puncak Jaya glaciers, is shown at 1:1,000,000 scale in figure 8. The major ice fields appear just above the center of the scene, with the small ice field on Ngga Pilimsit about 12 km west of these. The glaciers are discernible on all MSS bands but are most clearly delineated on the near-infrared MSS bands 6 and 7. On MSS bands 4 and 5 it is difficult to distinguish the ice from unvegetated limestone, which also has a high reflectivity. This is particularly noticeable around Ngga Pilimsit, even on MSS band 7 (fig. 8). The Ngga Pilimsit ice body consists of a small ice cap, several hundred meters in diameter, on the summit, plus a similar-sized glacier on a ledge below and to the southwest of the summit (fig. 9). Only the lower ice field can be distinguished from the surroundings on MSS band 7 (fig. 8), although there is a slight variation in the gray scale between the summit ice and the surroundings on MSS band 6 (fig. 10).

A Landsat MSS false-color composite (bands 4, 5, and 7) of this scene has been examined, but, in general, it shows less than separate examination of the individual bands. The MSS band 7 image best displays the area surrounding the ice fields. The glaciers are at an elevation of more than 4,300 m astride the crestal ridges of this part of the central range of New Guinea. To the south the elevation decreases abruptly within a distance of 40 km to the lowland swamps, which extend to the Arafura Sea 50 km farther south. The southern face of the range is carved by gullies of the predominantly north-south drainage system. To the north the land surface falls more gradually, and high grassy plateaus, more than 3,000 m in elevation, extend east-west immediately north of the divide.

Large morainal ridges can be seen immediately north of the ice fields of the Puncak Jaya region shown in figure 8, extending up to 5 km onto the Kemabu Plateau. These remnants of the youngest Pleistocene glaciation (Wisconsinan, or Würm) can be mapped directly from the Landsat image and show a distribution very similar to that given on the CGE 1:250,000-scale map sheet cited previously. Minor differences between the two maps are largely due to discrepancies in the base map for the CGE sheet. Similarly, a plot from the Landsat image of the prominent lakes on the plateau, and the river courses, shows minor discrepancies in the 1:1,000,000-scale Royal Australian Air Force (RAAF) Operational Navigation Chart of the region (ONC M–13, edition 4, 1973).

The present-day ice-covered areas are shown in more detail in figure 10. MSS band 6 provides the clearest delineation of the ice, although we have also made extensive use of the MSS band 7 image. Even the Southwall Hanging Glaciers, less than 100 m in the north-south dimension, are clearly shown on the image.

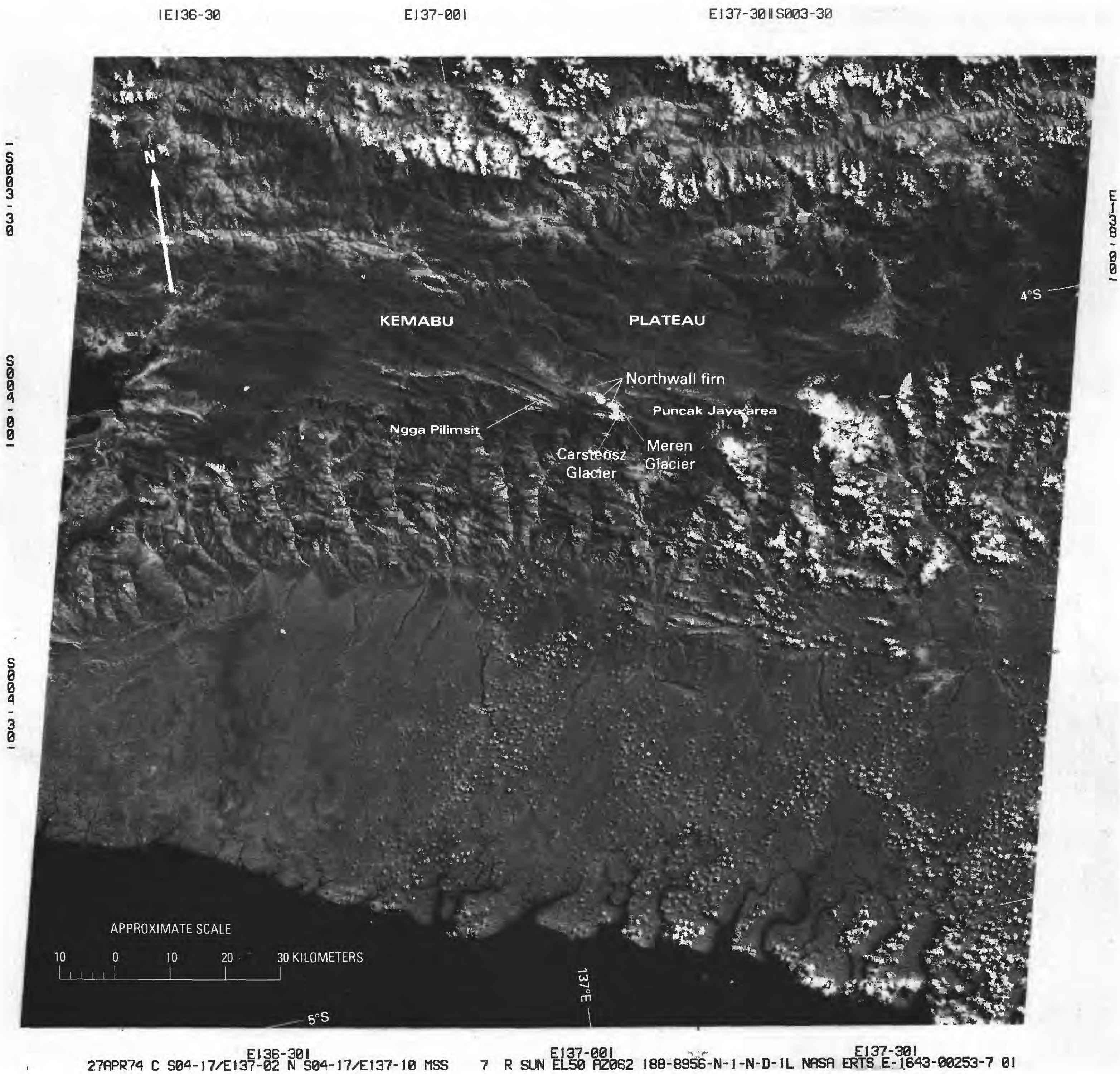

Figure 8.—*Landsat 1 image (1643–00253, band 7; 27 April 1974) showing the ice fields of the Puncak Jaya region (near center). The strike of the bare limestone outcrops that form the crestal ridge is west-northwest. To the north of the glaciers is the glacial-drift-veneered limestone Kemabu Plateau and, at the bottom of the image, the Arafura Sea. NASA Landsat image from the EROS Data Center.*

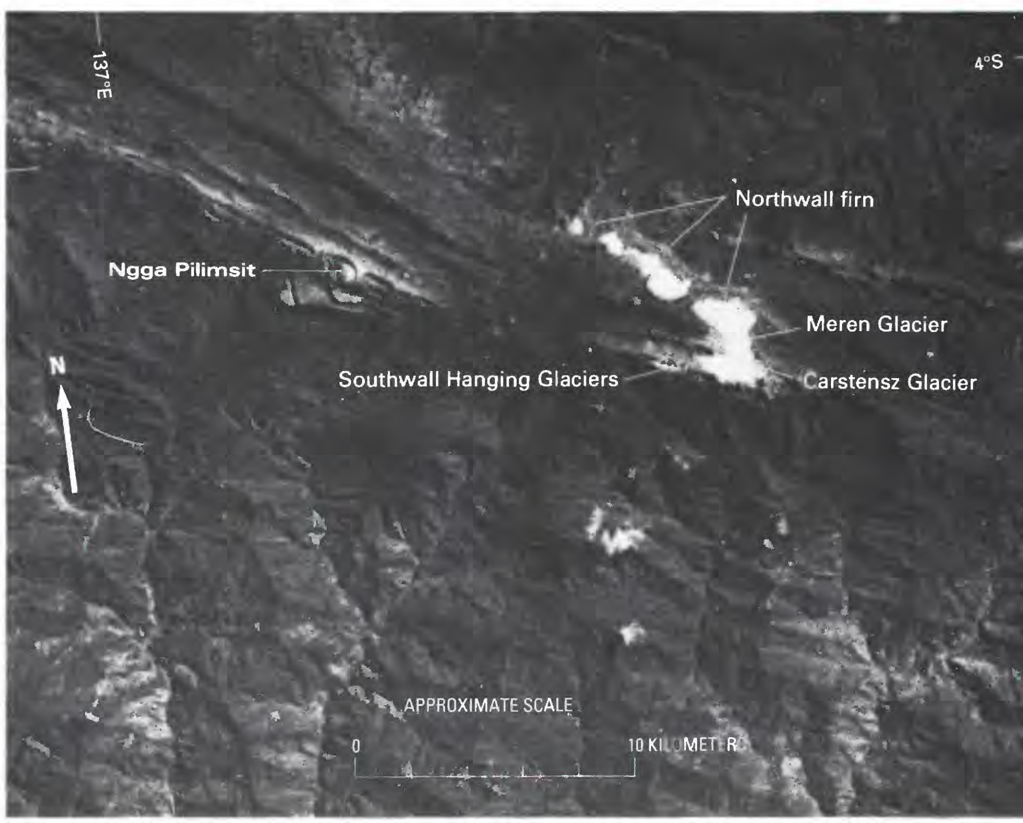

***Figure 9.**—Oblique aerial photograph looking east at the Ngga Pilimsit ice cap in 1972. In 1942 the summit ice dome and the lower glacier were joined. Photograph acquired during the Carstensz Glaciers Expeditions (CGE).*

***Figure 10.**—An approximately 1:275,000-scale enlargement of part of a Landsat 1 image (1643–00253, band 6; 27 April 1974) showing the Puncak Jaya glaciers (right) and Ngga Pilimsit (left).*

In our analysis we have used only standard Landsat photographic products, and not digital data or photographic images with enhanced gray scales. A map of the 1974 ice extent (fig. 11) has been produced by using both simple optical enlargement of the image and density contours produced from the image by using a scanning microdensitometer. Similar techniques were used by Krimmel and Meier (1975) for the study of South Cascade Glacier, Washington State, U.S.A.

Ice and snow boundaries were first traced from a 1:1,000,000-scale positive transparency optically enlarged to a scale of 1:20,000. All four MSS bands were used to derive a resultant "composite minimum brightness" map: that is, only those areas that appeared light on all four bands were plotted as glacierized on the final map. As noted previously, MSS bands 6 and 7 gave a minimum ice area. Although this technique is highly subjective, and the observer did use knowledge of the local terrain to interpret the images, it did reveal several interesting features when compared with the 1972 ice boundary shown in figure 2.

***Figure 11.**—Satellite-derived boundary of the Puncak Jaya glaciers in 1974 compared with the 1972 CGE boundary. Inset shows the 1974 boundary of the Ngga Pilimsit ice cap, 12 km west-northwest of Puncak Jaya. (See text section "Observation and Mapping of the Glaciers Shown on Landsat Images" for a discussion of the method used to produce the figure.)*

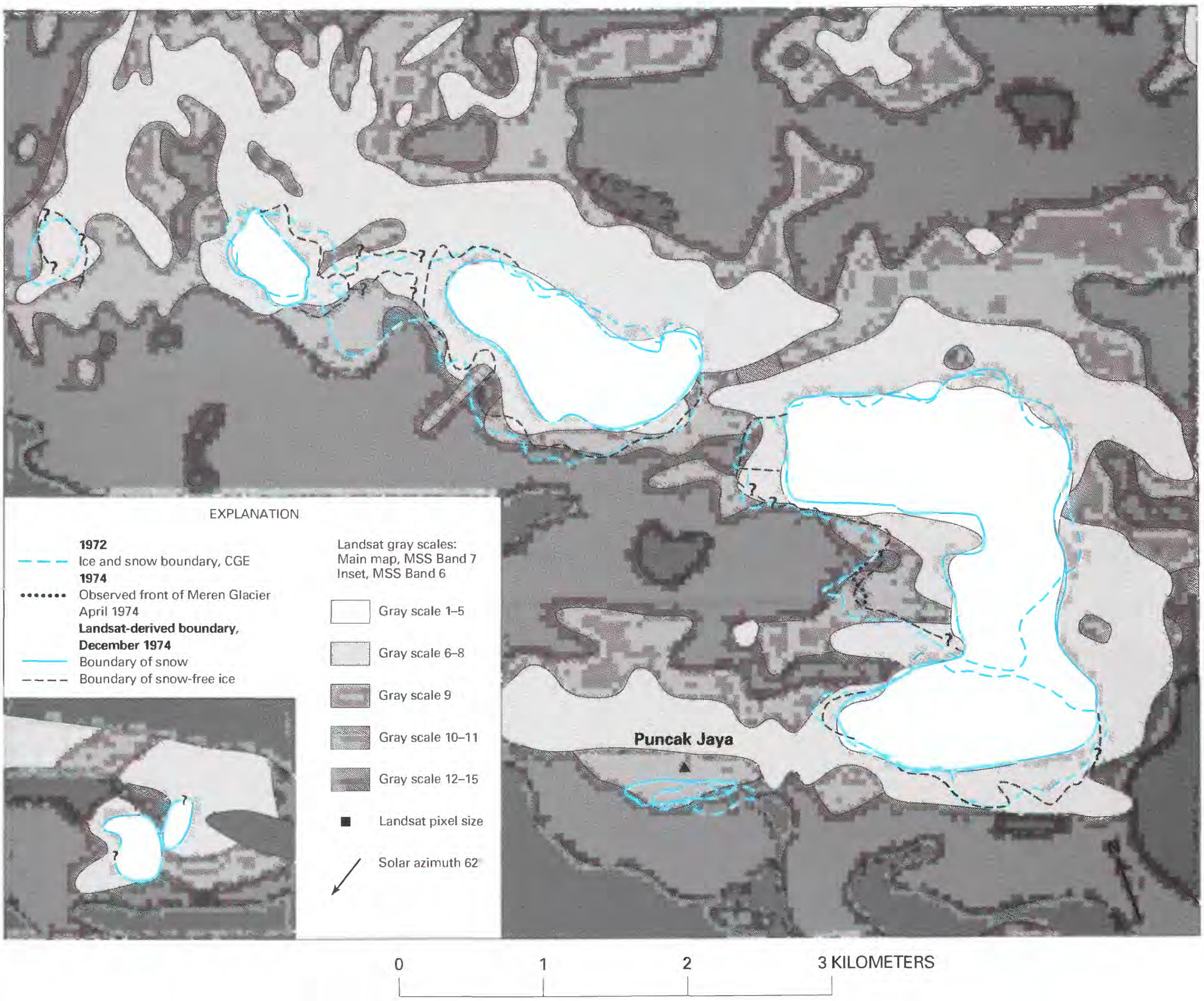

Along the northern edge of the eastern section of the Northwall Firn, the ice boundary is conterminous with the tops of high cliffs, and mass-balance changes do not lead to changes in the shape of the ice margin. Here the satellite-derived ice margin is very similar in shape and position to the margin as plotted photogrammetrically from the 1942 air photographs. The excellent agreement at these points is an indication of the accuracy and resolution obtainable from the Landsat image. The far western end of the Northwall Firn, however, does not correlate well on the two plots, although the positions are similar. This is thought to be due to errors in the CGE map, because this ice margin was determined only from oblique aerial photographs. Similarly, there are discrepancies along the eastern ice border, also limited by precipitous cliffs, and the least accurate region of the CGE map.

On both MSS bands 6 and 7, the ablation zone appears considerably darker on the Meren Glacier than on the other ice fields. The Meren snout supports a heavy population of cryoalgae (Kol and Peterson, 1976) and is riddled with englacial lakes (Peterson, 1976). These features lower the surface reflectivity, and an apparent snowline is evident on the Meren at elevations of between 4,550 and 4,650 m. This compares with the equilibrium-line elevation determined in 1972 as 4,580 m. There is some indication of a snowline, although not as obvious, in other areas where the cryoalgae are not as concentrated.

There is also some evidence of continued glacier retreat, from the satellite observations. The terminus of the Meren Glacier appears to have retreated about 200 m, and the large central part of the Northwall Firn appears to have separated further into two independent firn fields, or at least into two sections joined by a thin band of snow-free ice. The retreat of the Meren Glacier is confirmed by a single ground observation made in December 1974, 8 months after the satellite image was obtained, which showed a retreat of 185 m since 1972 (R. Mitton, pers. commun.) but a slightly different terminus shape than that derived from the Landsat image (fig. 8).

The 1981 vertical aerial photography obtained during the combined Indonesian and Australian mapping, although taken after a fresh snowfall, also suggests that the central Northwall Firn had separated into two parts after 1972, and this separation is clearly seen in a recent, but undated, oblique aerial photograph (Dick and Fenwick, 1984).

As a more objective check on the ice edge, an MSS band 7, 1:1,000,000-scale positive transparency was scanned with a microdensitometer to produce the gray-scale contours shown in figure 11. The microdensitometer aperture was set to scan an area equivalent to 80 m by about 200 m on the ground (or about 1 by 2.5 times the size of Landsat picture elements (pixels)), and scans were made every 0.2 mm on the image (200 m on the ground) along the direction of the glacial valleys. The density contours plotted in figure 11 have been condensed from the 15 Landsat photographic gray-scale levels (1 = white, 15 = black).

The snow-covered areas are clearly delineated by Landsat gray-scale levels of 5 and less, but the interpretation of areas showing a level of 6 to 9 is more ambiguous. The image was made with a solar elevation angle of 50° and an azimuth of 62°. Steep, unvegetated limestone slopes facing the Sun, for example the eastern and northern walls and the north face of the Puncak Jaya massif, show a gray-scale level of 6 to 8. These slopes may also have a scattered snow cover (compare fig. 4). Elsewhere, for example on the ablation zone of the Meren Glacier and possibly in other areas near southern or western ice edges, gray-scale levels of 6 to 9 indicate bare ice. The unvegetated limestone, not directly sunlit, shows a level of 9 to 11, and lakes, or heavily shaded areas, a level of 11 to 12.

Because the Southwall Hanging Glaciers are less than 100 m wide, they do not show in the contours made from a scanning interval of 200 m, but they can be seen on the optically enlarged image.

The December 1974 ice boundary shown in figure 11 has been plotted from a combination of the density contours and the optical enlargement and is compared with the 1972 CGE ice boundary. The inset map of the Ngga Pilimsit ice cap, the first produced for that area, has been derived from the density contours of the MSS band 6 image. Table 2 shows the 1974 ice areas compared with 1972 areas, after the latter have been corrected for map errors revealed by the satellite data. Continued retreat of the ice fields between 1972 and 1974 is apparent.

TABLE 2. — *Ice areas (in square kilometers) in the Puncak Jaya region*

[Areas in parentheses include possible snow-free ice areas on the Northwall Firn]

	February 1972	April 1974
Northwall Firn	3.6	2.8 (3.0)
Meren Glacier	2.2	2.1
Carstensz Glacier (including Wollaston and Van de Water Glaciers)	1.4	1.4
Southwall Hanging Glaciers	.1	.1
Total	7.3	6.4 (6.6)
Ngga Pilimsit ice cap	--	.2

Puncak Mandala

Location and observation of the small Mandala ice field on Landsat imagery is not as simple as for the much larger Puncak Jaya glaciers or for the Ngga Pilimsit ice cap, which can be located relative to the Puncak Jaya glaciers. We have been able to use first-hand knowledge of the terrain features in the Puncak Jaya area when interpreting the Landsat images; we do not have such knowledge of Puncak Mandala.

Neither maps, such as the 1:1,000,000-scale U.S. Defense Mapping Agency Operational Navigation Chart, ONC M-13, nor the latitude and longitude gridding on the primary Landsat image products is accurate enough to locate Puncak Mandala by absolute geographical position. We can, however, locate the region relative to the extensive drainage net of the Sungai Pulau (Einlanden River), which shows similar features on the images and map (although separated by about 11 km in absolute position near Puncak Mandala). This drainage net, on the southern slopes of the New Guinea cordillera, shows up most clearly in images obtained during February, March, and April, when the rivers are swollen following the southwest monsoons.

Identification of the ice field is further complicated by light-colored limestone (especially where recently deglaciated), short-lived snowfalls, and even the smallest convective or orographic clouds, which are common and are often as large as or larger than the ice cap. The Puncak Mandala ice cap can, however, be identified on Landsat images of 19 August 1981, 21 March 1983, and 3 January 1984 (although there is also new snow in the last scene) (table 1). While the imagery confirms the continued existence of this very small ice cap, we do not believe that the imagery can be used either to map or to record changes in the ice field without ground-observation data for the region.

Changes in the Puncak Jaya Glaciers, 1974 to 1983

The recent images obtained by the Australian Landsat Station (table 1) allow continued monitoring of fluctuations of the Puncak Jaya glaciers. Examination of the images for 8 September 1982 and 19 March 1983 shows no significant change in extent of the ice fields since 1974, meaning that no change in ice edge of greater than 100 m has occurred. Separation of the Northwall Firn into four independent firn fields is confirmed by these images, but even the smallest, western portion of the Northwall Firn and the Southwall Hanging Glaciers are largely unchanged since 1974. The low albedo of the ablation zone of the Meren Glacier makes it difficult to distinguish the ice from recently deglaciated limestone in front of the glacier.

Allison and Kruss (1977) used a numerical model of glacier dynamics to simulate the extensive retreat of the Meren and Carstensz Glaciers observed between 1936 and 1972. They attributed that retreat to a rise in air temperature of about 0.6 °C per century since around 1850. The decrease in glacier-retreat rate between 1974 and 1983 does not, however, suggest a reversal or cessation of this warming: the model results predicted that, despite continued warming at the above rate, the glacier-retreat rates would decrease after about 1975.

While not in immediate danger of disappearing altogether, it would appear that the Meren and Carstensz Glaciers, the only true valley glaciers in New Guinea, are becoming relatively simple firn fields or ice caps and are becoming less sensitive to climatic variations.

Conclusion

Landsat MSS images offer the possibility of monitoring glaciers as small as those on the Puncak Jaya massif and of identifying the even smaller ice masses of Ngga Pilimsit and Puncak Mandala.

The Landsat imagery can be used to monitor glacier retreat (or advance), to correct errors in existing maps, and possibly to give a gross indication of the mass balance from the snowline elevation, which, in this region, varies little seasonally. We must stress, however, that proper interpretation of the images requires knowledge of the terrain from ground studies. Although obviously lacking the resolution of aerial photographs, the Landsat images offer greater frequency of coverage, consistency of data, and, for these equatorial regions, uniformity of illumination (Sun angle). Provided proper and adequate ground truth is available, even more detailed information could be obtained from analysis of the Landsat digital data or by the use of the higher resolution Landsat thematic mapper data.

Acknowledgments

The authors acknowledge the consistently helpful and patient support of staff of the Australian Landsat Station in directing us to the most suitable imagery, and both H.M.S. Hartono, Director, Indonesian Geological Research and Development Centre, and David Trail, Bureau of Mineral Resources, Australia, Irian Jaya Geological Mapping Project, for making available the 1976 and 1980 aerial photographs.

References Cited

Allison, I., 1975, Morphology and dynamics of the tropical glaciers of Irian Jaya: Zeitschrift für Gletscherkunde und Glazialgeologie, v. 10 (1974), no. 1-2, p. 129-152.

———1976, Glacier regimes and dynamics, *in* Hope, G.S., Peterson, J.A., Radok, U., and Allison, I., eds., The equatorial glaciers of New Guinea: Rotterdam, A.A. Balkema, p. 39-59.

Allison, I., and Bennett, J., 1976, Climate and microclimate, *in* Hope, G.S., Peterson, J.A., Radok, U., and Allison, I., eds., The equatorial glaciers of New Guinea: Rotterdam, A.A. Balkema, p. 61-80.

Allison, I., and Kruss, P., 1977, Estimation of recent climate change in Irian Jaya by numerical modeling of its tropical glaciers: Arctic and Alpine Research, v. 9, no. 1, p. 49-60.

Allison, I., and Peterson, J.A., 1976, Ice areas on Mt. Jaya: Their extent and recent history, *in* Hope, G.S., Peterson, J.A., Radok, U., and Allison, I., eds., The equatorial glaciers of New Guinea: Rotterdam, A.A. Balkema, p. 27-38.

Anderson, E.G., 1976, Topographic survey and cartography, *in* Hope, G.S., Peterson, J.A., Radok, U., and Allison, I., eds., The equatorial glaciers of New Guinea: Rotterdam, A.A. Balkema, p. 15-25.

Dick, G., and Fenwick, J., 1984, Where the ice age lingers: Panorama, no. 31, p. 9-15 (Ansett Airlines in-flight magazine).

Dozy, J.J., 1938, Eine Gletscherwelt in Niederlandisch-Neuguinea: Zeitschrift für Gletscherkunde, v. 26, no. 1-2, p. 45-51.

Garren, W.R., Peterson, B.D., and Page, C.R., 1982, Gazetteer of Indonesia (3d ed.): Washington, D.C., Defense Mapping Agency, 2 v., 1529 p.

Hope, G.S., and Peterson, J.A., 1976, Palaeoenvironments, *in* Hope, G.S., Peterson, J.A., Radok, U., and Allison, I., eds., The equatorial glaciers of New Guinea: Rotterdam, A.A. Balkema, p. 173-205.

Kol, E., and Peterson, J.A., 1976, Cryobiology, *in* Hope, G.S., Peterson, J.A., Radok, U., and Allison, I., eds., The equatorial glaciers of New Guinea: Rotterdam, A.A. Balkema, p. 81-91.

Krimmel, R.M., and Meier, M.F., 1975, Glacier applications of ERTS images: Journal of Glaciology, v. 15, no. 73, p. 391-401.

Mercer, J.H., 1967, Glaciers of New Guinea, *in* Southern hemisphere glacier atlas: Technical Report 67-76-ES by the American Geographical Society, New York, for the Earth Sciences Laboratory, U.S. Army Natick Laboratories, Natick, Massachusetts, Series ES-33, June, p. 197-207.

Müller, F., 1977, Fluctuations of glaciers, 1970-1975: Paris, International Association of Hydrological Sciences, UNESCO, 269 p.

Peterson, J.A., 1976, The lakes, *in* Hope, G.S., Peterson, J.A., Radok, U., and Allison, I., eds., The equatorial glaciers of New Guinea: Rotterdam, A.A. Balkema, p. 93-112 (includes appendices by I.A.E. Bayly, p. 107-110 and Joan Powling, p. 111).

Peterson, J.A., Hope, G.S., and Mitton, R., 1973, Recession of snow and ice fields of Irian Jaya, Republic of Indonesia: Zeitschrift für Gletscherkunde und Glazialgeologie, v. 9, no. 1-2, p. 73-87.

Glaciers of Irian Jaya, Indonesia, and New Zealand—

GLACIERS OF NEW ZEALAND

By TREVOR J.H. CHINN

SATELLITE IMAGE ATLAS OF GLACIERS OF THE WORLD

Edited by RICHARD S. WILLIAMS, Jr., *and* JANE G. FERRIGNO

U. S. GEOLOGICAL SURVEY PROFESSIONAL PAPER 1386–H–2

Landsat images, in conjunction with aerial photographs and field measurements, were used to monitor changes in the transient snowline and the largest glaciers of New Zealand

UNITED STATES GOVERNMENT PRINTING OFFICE, WASHINGTON : 1989

CONTENTS

GLACIERS OF IRIAN JAYA, INDONESIA, AND NEW ZEALAND—

GLACIERS OF NEW ZEALAND

By TREVOR J.H. CHINN[1]

Abstract

Glaciers occur on the North Island on Mount Ruapehu and on the South Island along the crest of the Southern Alps from the Spenser Mountains in the north to southern Fiordland in the south. New Zealand has a humid maritime climate. The prevailing westerly winds bring 3,000 mm of annual precipitation to the western coastal plains, 15,000 mm to just west of the main divide, and 1,000 mm to the eastern ranges. Easterly and southerly winds are important sources of snow east of the main divide. A comprehensive glacier inventory that has just been completed indicates that the total number of glaciers exceeding 0.01 km^2 in area in the Southern Alps is about 3,155, with an estimated volume of 53.3 km^3 and an area of 1,159 km^2. There are six glaciers on Mount Ruapehu. The first published descriptions of New Zealand glaciers occurred in 1859. Early visitors made observations on positions of termini and rates of movement of the glaciers, and, in 1889, the first precise measurements were carried out. Modern studies began in the 1950's and included studies of flow, fluctuation, and mass and water balance on individual glaciers. The mapping of glaciers began with sketches of Franz Josef Glacier in 1865. The first maps were produced in the 1890's. Topographic mapping of the entire country at a scale of 1:63,360 with 100-ft contours was begun in 1958 and completed in the 1970's. Currently the Department of Survey and Land Information is preparing a new series at a scale of 1:50,000 with a 25-m contour interval. Aerial photographs of all glacierized areas are available; Landsat images cover all the areas, but not all the images are useful for glacial observations because of cloud cover or seasonally incorrect acquisition dates. Landsat images are more appropriate for studies of the larger glaciers, because the spatial resolution of the image is inadequate for glaciers smaller than about 1.0 km^2. However, Landsat imagery is useful in many cases in New Zealand for determining the rate and direction of glacier flow, changes in glacier snowline and margins, and past glacier extent on the basis of morainal sequences.

Introduction

New Zealand comprises three main islands situated between 34° S. and 47° S. latitude. North Island has extensive areas of low mountain and hill country of Mesozoic and Tertiary sediments and a number of prominent volcanic cones. The mountains barely reach above the present vegetation limit, and the scant evidence available suggests that glaciers possibly did occur on the highest of these ranges during the Pleistocene. Three of the highest of the volcanic cones reach close to the permanent snowline, but only Mount Ruapehu, whose summit is at 2,752 m, supports snowfields, which form six glaciers.

[1] New Zealand Geological Survey, University of Canterbury, Private Bag, Christchurch, New Zealand.

South Island is more mountainous than North Island, and the boundary between the Pacific and Indian plates cuts diagonally through the island from southwest to northeast as the New Zealand Alpine fault. Toward the northeast, the single fault splinters into a number of faults. Vertical and dextral strike-slip movements continue and have rapidly uplifted the young, steep mountains east of the fault line, with lesser uplift to the west and north of the fault line. Rock types may be roughly divided into three simple categories: crystalline plutonic rocks of Fiordland in the southwest; schist in the central south, which wedges out northward adjacent to the fault; and sandstone to the east and north of the schist.

Average peak summits range from 1,850 m in Fiordland to 3,000 m in the central Southern Alps (Mount Cook, the highest, reaches 3,764 m) and descend to 2,000 m in the north-central Southern Alps. To the northeast young blocks of the Kaikoura Ranges reach to over 2,700 m, but because they receive little precipitation these peaks do not support glaciers (fig. 1). Stewart Island presently supports no glaciers, although small glaciers were present during the Pleistocene.

New Zealand has a humid maritime climate, with the Southern Alps lying across the path of the prevailing westerly winds. This situation creates steep, eastward precipitation gradients and a strong föhn effect. Mean annual precipitation rises rapidly from 3,000 mm along the narrow western coastal plains to a maximum of 15,000 mm or more in the western part of the Southern Alps a few kilometers west of the main divide. From this maximum, precipitation diminishes approximately exponentially to about 1,000 mm in the eastern ranges (Griffiths and McSaveney, 1983; Chinn, 1979). Although westerly winds prevail, easterly and, more especially, southerly winds are important sources of snow to the east of the main divide. Precipitation is evenly distributed throughout the year.

Occurrence of Glaciers

Glaciers of the Southern Alps occur either in groups or singly from southern Fiordland in the south to the Spenser Mountains in the north (fig. 1). Several active rock glaciers occur on the inland Kaikoura Ranges. North of the Arthur's Pass area there are only a few small glaciers and permanent snow patches.

The glaciers of the Southern Alps may be divided into four glacial regions containing groups of the larger glaciers (fig. 1). To the north, the Mount Whitcombe region includes the large Ramsay and Lyell Glaciers, together with the ice plateau of the Bracken Snowfield, and extends south to include the dual snowfields of the Garden of Eden and the Garden of Allah (fig. 2). The Mount Cook region contains the largest glaciers of the Southern Alps. These include the Godley, Classen, Murchison, Tasman, Hooker, and Mueller Glaciers east of the main divide, and the Franz Josef and Fox Glaciers (Sara, 1968) to the west. Farther south, the Mount Aspiring region has some extensive névé-sheathed slopes surrounding Mount Aspiring and two main glaciers, the Bonar and Volta. The Olivine Ice Plateau and adjacent valley glaciers south of Mount Aspiring are included in this region. The Mount Tutoko region, the southernmost region, encompasses the north Fiordland and central Fiordland glaciers.

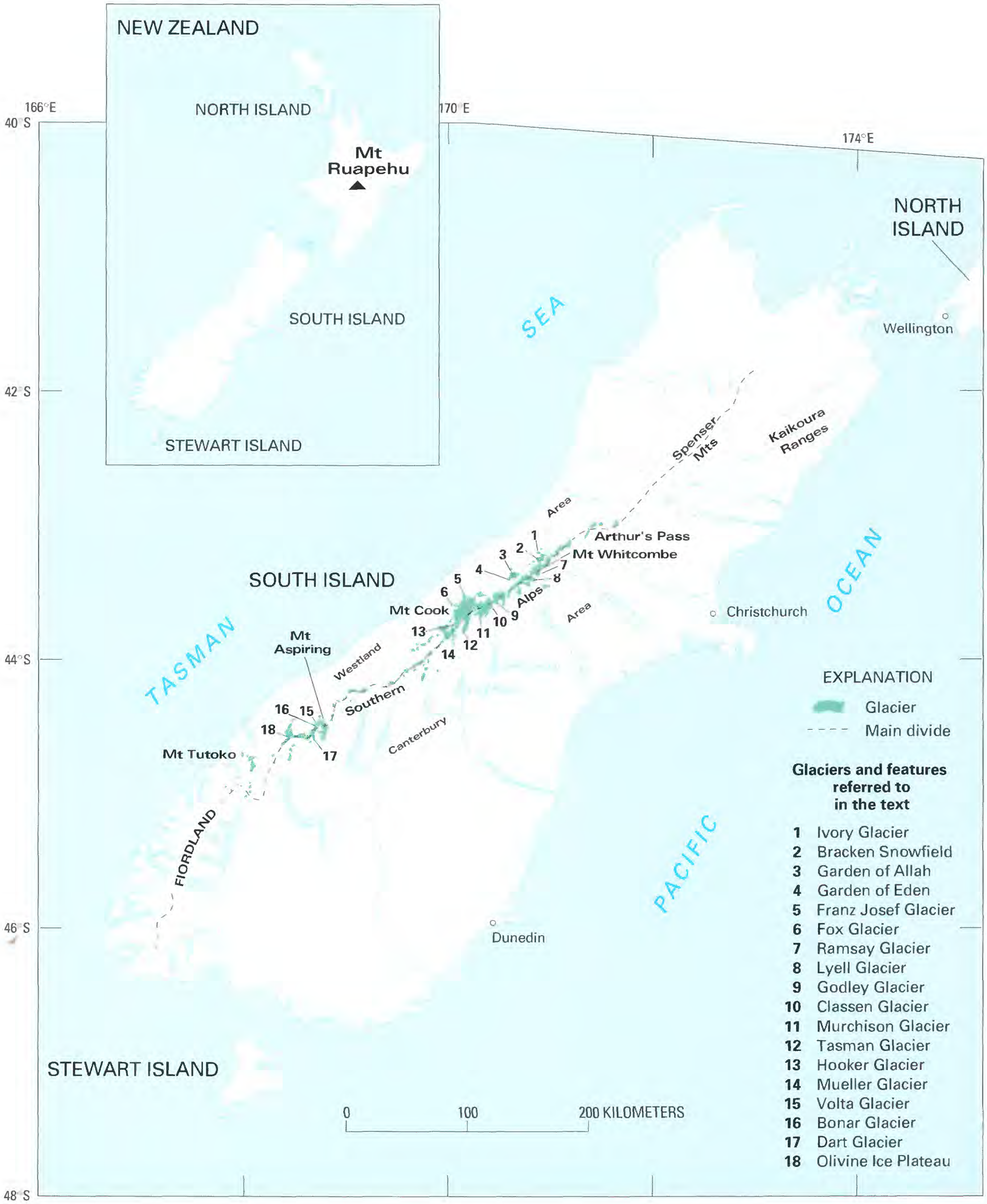

***Figure 1.**—Location map showing glacial regions and locations of glaciers mentioned in the text.*

Anderton (1973) had previously identified 527 glaciers more than 0.1 km^2 in area and estimated the volume of water stored as perennial snow and ice in the glaciers of the Southern Alps to be approximately 50 km^3, with an area of 810 km^2. Results from the present glacier inventory indicate that the total number of glaciers exceeding 0.01 km^2 in area in the Southern Alps is 3,155, with an estimated ice volume of 53.3 km^3 and a total glacier area of 1,159 km^2. In the Mount Whitcombe region 819 glaciers have been inventoried; 351 of these occur to the west of the main divide (Westland area) and the remaining 468 to the east of the main divide (Canterbury area). Many glaciers have areas close to 0.2 km^2, and 82 percent of the Canterbury glaciers are this size or smaller (fig. 3), while in Westland 70 percent of the glaciers are equal to or less than 0.2 km^2 (fig. 4). Fifty percent of Canterbury glaciers are smaller than 0.06 km^2, while 50 percent of Westland glaciers are smaller than 0.09 km^2. Canterbury glaciers predominantly face south to southeast, and most Westland glaciers face between west and north (fig. 5).

Figure 2.*—Oblique aerial photograph looking northeast on 22 March 1983 at the Garden of Eden, an ice field that has numerous outlet glaciers. A second ice field, the Garden of Allah, is visible behind the ridge separating the two névés. Photograph by Trevor J.H. Chinn, New Zealand Geological Survey, slide A 42–29.*

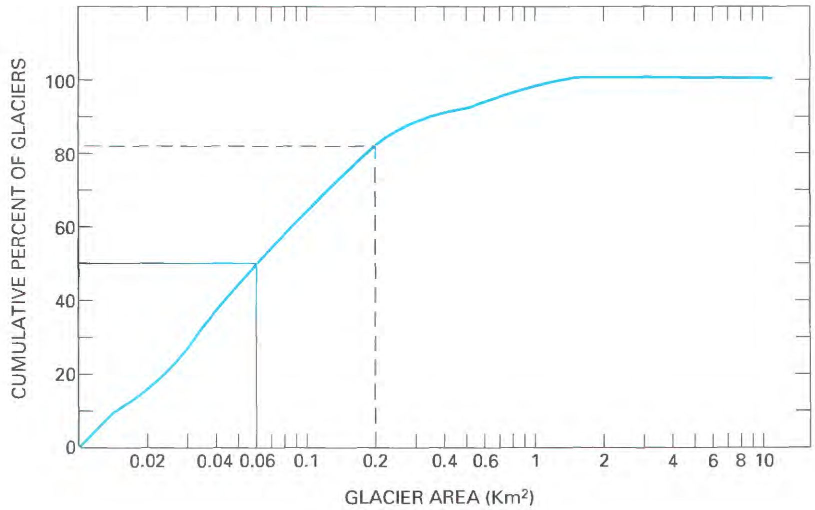

***Figure 3.**—Distribution by size of 468 Canterbury glaciers of the Mount Whitcombe region. Fifty percent of all glaciers of this region are less than 0.06 km² in area, and 82 percent are less than 0.2 km².*

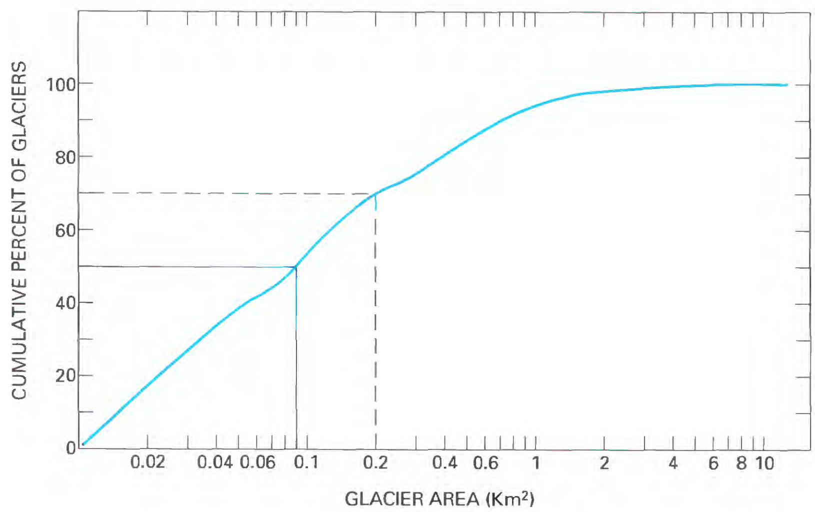

***Figure 4.**—Distribution by size of 351 Westland glaciers of the Mount Whitcombe region. Fifty percent of all glaciers of this region are less than 0.09 km² in area, and 70 percent are less than 0.2 km².*

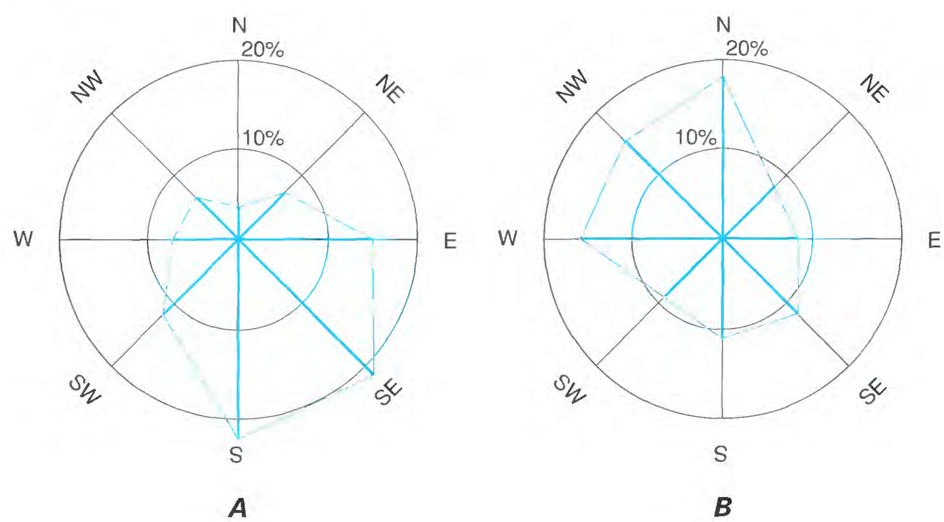

***Figure 5.**—Aspect rose diagrams of 819 glaciers of the Mount Whitcombe region.* A, *Canterbury glaciers (east of main divide);* B, *Westland glaciers (west of main divide).*

Observation of Glaciers

Historical Glacier Observations

The first Europeans who might have seen the glaciers of the Southern Alps were the explorers Abel Tasman (in 1642) and Captain James Cook (in 1769), when they sailed along the West Coast of New Zealand, although neither of them mentioned seeing glaciers. The first published description of a New Zealand glacier appears to be of the Franz Josef Glacier, recorded in the log of the *Mary Louisa* when sailing off the West Coast in 1859, and subsequently published in the Lyttelton (New Zealand) Times, 6 July 1859 (Sara, 1970).

Descriptions of glaciers become abundant in the 1860's, soon after the discovery of gold stimulated extensive exploration and prospecting in alpine regions, especially on the West Coast. The earliest systematic records of glaciers appear in the journals and reports of C.E. "Mr. Explorer" Douglas and A.P. Harper. From the late 1860's onward Douglas explored and carefully reported on most of the notoriously impenetrable West Coast valleys (Pascoe, 1957). Later, mainly in the 1890's, A.P. Harper carried out a tremendous amount of exploration work for the Department of Lands and Survey, frequently in the company of Douglas (Harper, 1896 and 1946). Harper was also a mountaineer and explored many of the glaciers on the eastern side of the ranges. Further systematic records of the glaciers appear in the New Zealand Alpine Journal, first published in 1892.

Early volumes of the New Zealand Alpine Journal contain accounts of the visits of Julius von Haast to the headwaters and glaciers of Rakaia and Rangitata Rivers in 1861, and to Tasman, Hooker, and Mueller Glaciers in 1862. In 1865, von Haast made the first sketch of Franz Josef Glacier, and its terminus was first photographed in 1867 by T. Pringle (Sara, 1970). Throughout the 1860's to the 1880's the headwaters of the main rivers on the eastern side of the Alps were visited by explorers, while Douglas systematically explored each of the rugged forested valleys of the west to its headwaters glaciers. By 1900, guided tours were being conducted from both sides of the Alps on Franz Josef and Tasman Glaciers.

Many of these early visitors made observations on the positions of the glacier termini and on rates of ice movement (Mannering, 1891; FitzGerald, 1896). In 1889, T.N. Brodrick began mapping topography and glaciers in the Mount Cook area (Gellatly, 1985). Cross-glacier lines of stakes were installed on Tasman, Murchison, and Hooker Glaciers, while painted stones were positioned in a line across Mueller Glacier. This work was the first precise glaciological measurement carried out in New Zealand. These sections were resurveyed in 1962 (Skinner, 1964). Observations of the positions of the termini of Franz Josef and Fox Glaciers by surveys and photographic records have been sporadically maintained since 1894 (fig. 6), and occasional measurements of rates of movement have been made (Bell, 1910; Speight, 1939). During the past two decades, National Park staff have taken weekly photographs from fixed points, giving a permanent time-lapse record of all fluctuations of glacier termini.

__Figure 6.__—Measured variations in the position of the termini of the Fox, Franz Josef, and Ivory Glaciers.

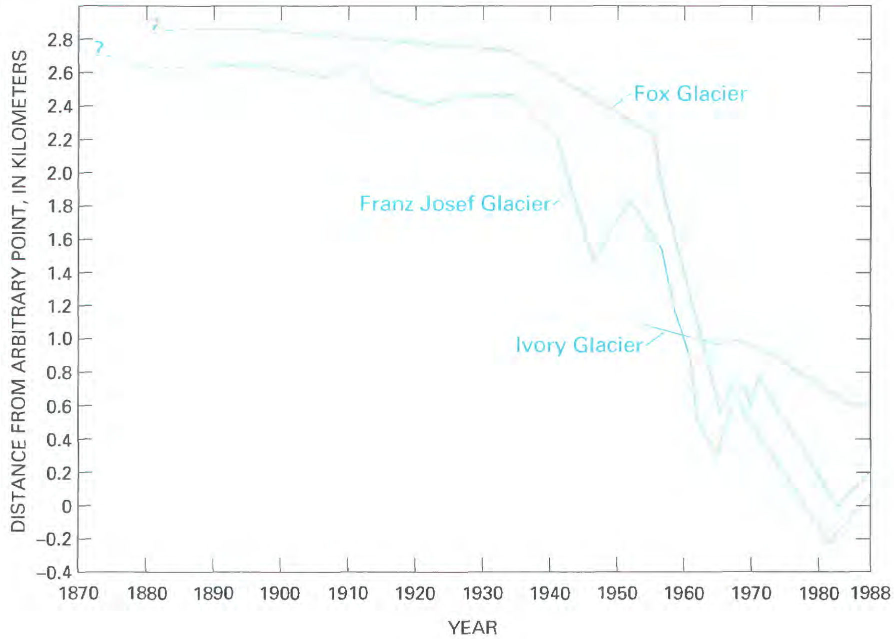

Modern Glacier Observations

In 1957, I.C. McKellar of the New Zealand Geological Survey began measuring movement and ice stratigraphy on Tasman Glacier (Goldthwait and McKellar, 1962). In 1965, when this initial project was completed, the Ministry of Works initiated mass-balance measurements; this work continued until 1973 (Chinn, 1969). In 1972, ice thickness was measured over three sections across the trunk of the glacier (Anderton, 1975). Repetitive oblique photographs are being made from time to time by the Mount Cook National Park Board. A recent study has documented the retreat of the small, steep Stocking Glacier, situated between Mueller and Hooker Glaciers (Salinger and others, 1983). To the west, the fluctuations of Franz Josef and Fox Glaciers have been documented by Suggate (1950), Bowen (1960), Sara (1968, 1970), and Soons (1971), but flow measurements by Gunn (1964) and McSaveney and Gage (1968) are the most comprehensive of the studies made on the ice of these glaciers.

In 1968, T.J. Chinn of the Ministry of Works began mass- and water-balance studies on Ivory Glacier (fig. 7), a small glacier west of the main divide chosen as part of an International Hydrological Decade (I.H.D.) program of representative basin studies (Anderton and Chinn, 1978). These studies continued, along with energy-balance projects, until 1974. In 1975, G. Bishop of the New Zealand Geological Survey, Dunedin, commenced limited balance and movement studies on Dart Glacier in Otago; these studies continue. On North Island, retreat of the glaciers of Mount Ruapehu was described by Odell (1955) and Krenek (1959). Later, in 1960, permanent photographic stations were installed (Heine, 1962), and balance studies were made on Whakapapanui Glacier over 1968–69 (Thompson and Kells, 1973).

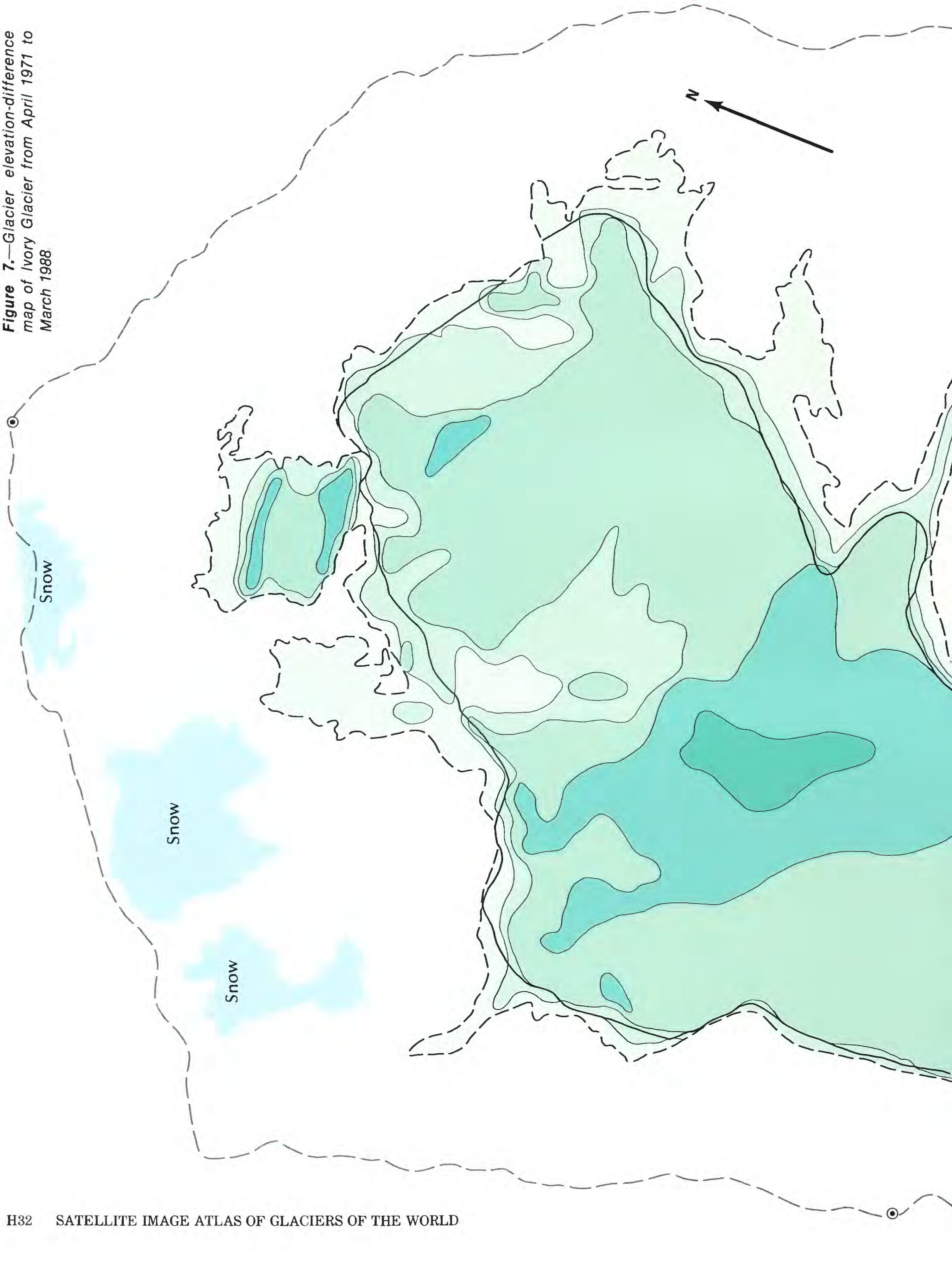

Figure 7.—Glacier elevation-difference map of Ivory Glacier from April 1971 to March 1988

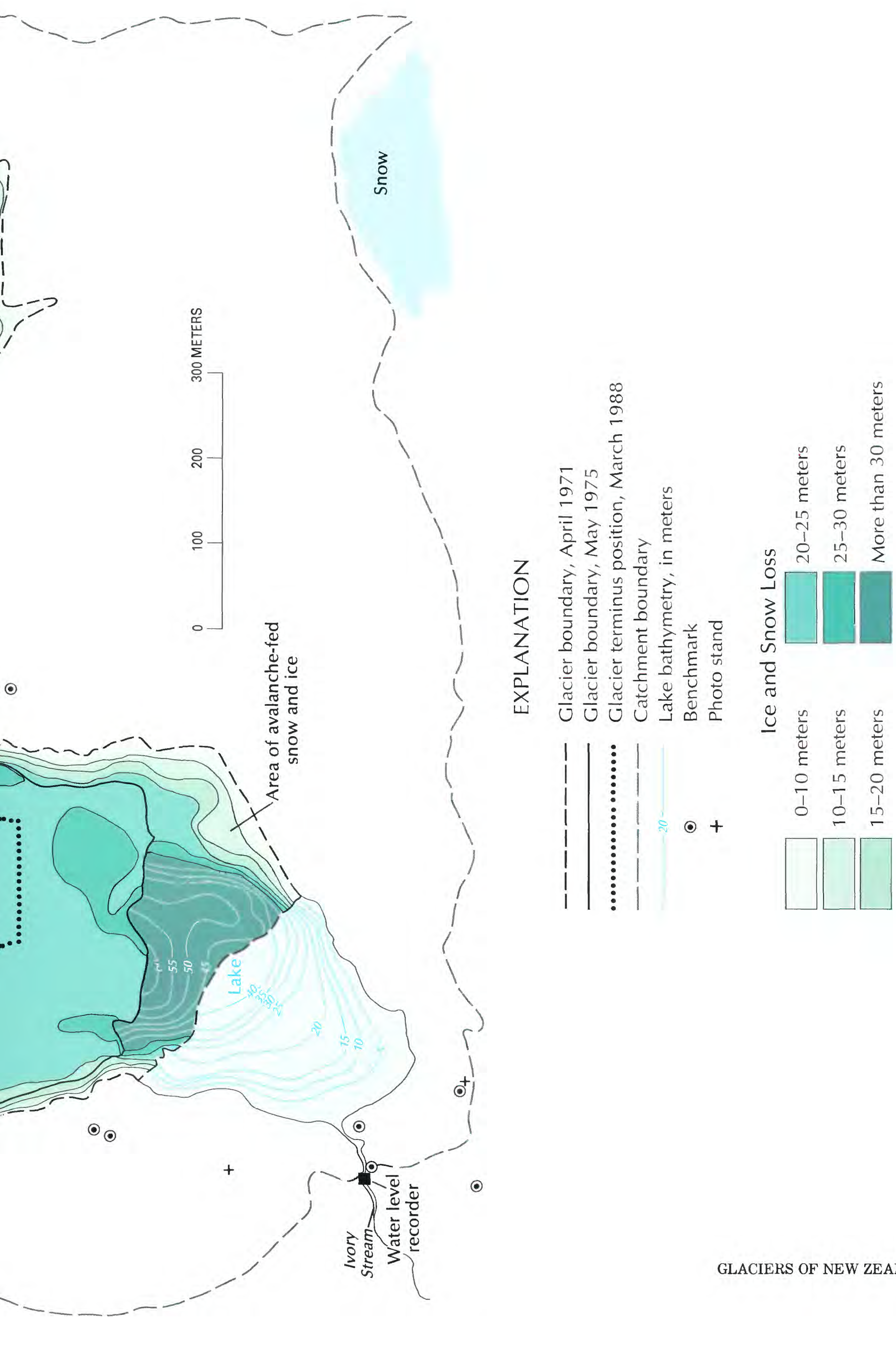
Snow
0
100
200
300 METERS
Area of avalanche-fed snow and ice
Lake
Ivory Stream
Water level recorder
EXPLANATION
Glacier boundary, April 1971
Glacier boundary, May 1975
Glacier terminus position, March 1988
Catchment boundary
Lake bathymetry, in meters
Benchmark
Photo stand
Ice and Snow Loss
0–10 meters
10–15 meters
15–20 meters
20–25 meters
25–30 meters
More than 30 meters

Glacier-snowline elevations (the elevation of the end-of-summer snowline on a glacier) are being measured in a program of annual photographic surveys of glaciers throughout the Southern Alps. The first complete survey was made in 1978 (Chinn and Whitehouse, 1980). Mean snowline altitudes varied from 1,500 m in the south and west to 2,200 m in the east. The trend of the snowline surface shows strongly the influence of westerly precipitation on the distribution of glaciers. Snowlines descend perceptibly from the extreme west to a trough located parallel to, but somewhat east of, the zone of maximum precipitation (Griffiths and McSaveney, 1983; Chinn, 1979). With decreasing precipitation, the snowline rises rapidly near the crest of the main divide and continues to rise with a lower eastward gradient. Imposed on this generalized pattern are complex topographic variations of two origins. Large mountain masses, lying across the direction of the prevailing northwest winds and west of the divide, generate precipitation-shadow areas, the result being higher snowlines in the shadow area. This pattern of precipitation-shadow areas is repeated east of the main divide. Where low passes occur, the precipitation-shadow effect is drastically reduced; moist maritime air masses, therefore, can penetrate east of the main divide, resulting in markedly lower snowlines than in the shadow areas.

Gradients of the snowline elevation across the main divide vary from 25 m km^{-1} to 40 m km^{-1}. These gradients are up to four times as steep as those found at the glaciation limit[2] (Porter, 1975) and 10 to 20 times as steep as those measured for arctic and subarctic regions (Andrews and Miller, 1972). Localized areas of very steep gradients occur that far exceed the mean values. The mean northeast to southwest gradient along the main divide is 1 m km^{-1}, or 115 m per degree of latitude.

Present glacial studies include the Dart Glacier work by the New Zealand Geological Survey, and photographic surveys being conducted by the staff of the Westland and Mount Cook National Parks. In addition, the Water and Soil Division of the Ministry of Works and Development has a New Zealand Glacier Inventory program in progress under the United Nations Educational, Scientific, and Cultural Organization (UNESCO) World Glacier Inventory project.

Mapping of Glaciers

Earliest Maps

Mapping of the main glaciers commenced early in the period of exploration. These maps are the result of the efforts of a few enterprising and capable individuals. The Franz Josef Glacier was sketched by von Haast in 1865, and, in 1893, Douglas and Harper compiled the first map. Fox Glacier was surveyed by Douglas and Wilson in 1894–95. The next maps were made by Greville and Bell in 1910 (Bell, 1910).

On the eastern side of the divide, almost all of the mapping work was concentrated in the Mount Cook area, where Julius von Haast made sketch plans of the Tasman, Godley, and Classen Glacier termini in the years 1862 and 1889 (Gellatly, 1985). In 1888, T.N. Brodrick began triangulation surveys and topographic mapping and produced a number of

[2] The lowest elevation in a given locality at which glaciers can develop and be sustained.

maps and plans of the Mount Cook and Godley Valley glaciers from 1889 until after the completion of his fieldwork in 1906.

In 1893, a topographic map of the "central portion of the Southern Alps" was published by the Royal Geographical Society, London. This map, showing the four large eastern glaciers and the two large western glaciers, was probably the first to show the relative positions of glaciers on both sides of the Alps. For the remainder of the Southern Alps, from the late 1890's, a series of survey district maps was produced to which details were added as exploration (mainly for pasture land) proceeded.

In Westland, before the turn of the century, there were practically no maps of the mountain areas apart from the sketches and maps of Douglas and Harper. The first reasonably reliable regional maps were base maps constructed in the early 1900's by the New Zealand Geological Survey as part of their geological surveys. These maps are rich in detail and show all glaciers observed, although the accuracy varied with the surveyor's proximity to the features mapped.

In 1911, a detailed map of the Franz Josef and Fox Glaciers was published by the Canterbury Progress League. This map, together with the 1893 map, was reprinted (unaltered) in 1976 in the New Zealand Alpine Journal with facsimile editions of early journal volumes.

Present Maps

No topographic maps of the glaciers were available until the Department of Lands and Survey commenced publishing a 1-inch-to-1-mile topographic maps series (New Zealand Mapping Series 1 at a scale of 1:63,360). Publication of the first sheets began in about 1958. Until this time, uncontoured 4-mile maps of the New Zealand Territorial Series (NZMS 10) at a scale of 1:253,440 and Survey District and County Series Cadastral Maps at 1:63,360 were the best available. By the mid 1970's, effectively the whole of New Zealand had been mapped in the 1:63,360-scale topographic series with a 100-ft contour interval. However, the glaciers depicted on some of these maps may not have accurate outlines in their upper areas. The maps were prepared from vertical aerial photographs on which the position of the névé boundary depends on the amount of snow, which in turn is dependent on the time of year that the photography was acquired. Most of the aerial photographic survey flight runs were not made at the correct time of year (optimum time is prior to the end-of-summer seasonal snow-cover minimum). As a result, these maps show variable amounts of snow cover. Thus, the earlier in the summer the photography, the greater the error in plotted glacier size. Attempts have been made to reduce this error, for example, on the Mount Cook Sheet (S. 79), where permanent snow boundaries have been based on data from local observations, rather than those shown on the aerial photographs. Currently, the Department of Survey and Land Information is preparing a series of maps at 1:50,000 scale and with a 25-m contour interval. This remapping program is a large undertaking, and it will be more than a decade before the new series is completed for the whole country. Data from the New Zealand glacier inventory are being used extensively in remapping the glacierized areas.

Imaging of Glaciers

Aerial Photography

The first known sequences of vertical aerial photographs in New Zealand were taken around 1937 and 1938 by New Zealand Aerial Mapping, Ltd., but these were mainly of lowland areas. A set of vertical aerial photographs was taken over the Franz Josef, Fox, Tasman, and Hooker Glaciers in 1953, followed by a most useful set of oblique aerial photographs taken by the Royal New Zealand Air Force along both sides of the Southern Alps in autumn 1955. These surveys were made just prior to the first of the systematic vertical aerial photographic flights made over the Southern Alps as part of a nationwide aerial photogrammetric mapping program. By the end of the 1960's all of the glacierized areas were photographed, and many areas have been rephotographed since.

Satellite Imagery

All of New Zealand's glacierized areas are included in existing Landsat images, but not all of the images are usable for glacial observations (fig. 8). The two requisites for an optimum usable image are no cloud cover and an image acquired at the time of minimum snow cover (late summer). Many of the better images of the glacierized areas have glacial features obscured by seasonal snow. The coding for each of the nominal scene centers shown on figure 8 refers primarily to the amount of cloud cover over the glacierized regions. Table 1 provides additional information on each image, including remarks about amount of snow cover.

Table 1 lists the known usable images of the New Zealand glaciers. Many additional images exist, but these are generally unacceptable because of excessive cloud cover or because of snow cover on winter scenes. Unfortunately, the Landsat satellite paths and image rows do not coincide well with the configuration of the glacierized areas. This results in images of the more important glacerized regions appearing at the margins of the images. The best available image of the Mount Cook area is the larger scale (1:500,000) Landsat 3 RBV image (30324–21342, subscene A), corresponding to the northwest quadrant of Path 79, Row 91, but this image lacks relief detail in the snowfields (Ferrigno and Williams, 1983).

Landsat images are more appropriate for the larger glaciers, because the spatial resolution of the image is inadequate for identifying details of small glaciers less than about 1 or 2 km^2 in area. On a 1:1,000,000-scale Landsat MSS image 1 km equals 1 mm, so a 1-km^2 glacier would measure 1 mm^2 on the image. Even on a 1:500,000-scale Landsat 3 RBV image, a 1-km^2 glacier would only be 4 mm^2. Unfortunately the rapid changes in small, steep, and very active glaciers, such as the one shown in figure 9, are difficult to monitor by satellite imagery. On some small glaciers the snowline has recently risen beyond the upper limits of the glacier, thereby leaving the entire glacier in the ablation zone (fig. 10).

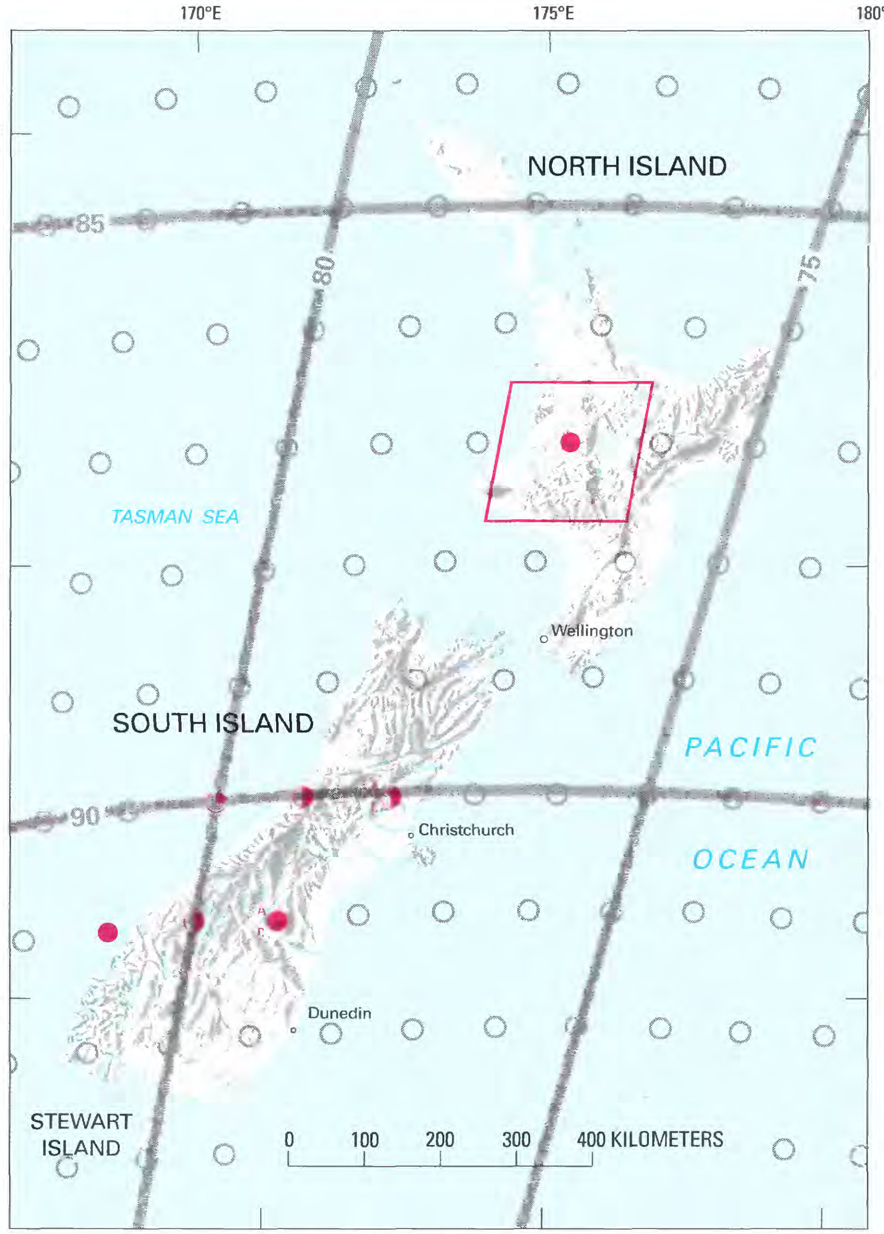

***Figure 8.**—Map of New Zealand showing availability of Landsat images of glaciers.*

EXPLANATION OF SYMBOLS

Evaluation of image usability for glaciologic, geologic, and cartographic applications. Symbols defined as follows:

- Excellent image (0 to ≤5 percent cloud cover)
- Good image (>5 to ≤10 percent cloud cover)
- Fair to poor image (>10 to ≤ 100 percent cloud cover)
- Unusable image (100 percent cloud cover)
- A B C D — Usable Landsat 3 return beam vidicon (RBV) scenes A, B, C, D refer to usable RBV subscenes
- Nominal scene center for a Landsat image outside the area of glaciers
- Approximate size of area encompassed by nominal Landsat MSS image. Landsat 3 RBV subscenes encompass slightly more than one overlapping quadrant (A, NW; B, NE; C, SW; D, SE) of an MSS nominal scene.

TABLE 1. — *Optimum Landsat 1, 2, and 3 images of the glaciers of New Zealand*

[See figure 8 for explanation of the symbols in the "Code" column]

Path-Row	Nominal scene center (lat.-long.)	Landsat identi-fication number	Date	Solar elevation angle (in degrees)	Code	Cloud cover (in percent)	Remarks
77–87	038° 49'S. 175° 21'E.	2389–21172	15 Feb 76	39	●	0	Marginal; fresh snow cover; North Island
78–90	043° 05'S. 172° 24'E.	2192-21265	02 Aug 75	15	◑	20	Snow cover in mountains; color composite available
78–90	043° 05'S. 172° 24'E.	30377–21275–A	17 Mar 79	30	◑	20	Landsat 3 RBV image
78–90	043° 05'S. 172° 24'E.	30377–21275–C	17 Mar 79	30	◑	20	Landsat 3 RBV image
79–90	043° 05'S. 170° 58'E.	1503–21421	08 Dec 73	50	◑	70	
79–90	043° 05'S. 170° 58'E.	2391–21300	17 Feb 76	36	◑	50	Good; some clouds
79–90	043° 05'S. 170° 58'E.	2409–21293	06 Mar 76	32	◑	20	Excellent; timed at minimum snow cover; some clouds
79–91	044° 30'S. 170° 25'E.	2787–21172	19 Mar 77	26	◕	10	Good; some clouds
79–91	044° 30'S. 170° 25'E.	2805–21163	06 Apr 77	21	●	0	Excellent; very good detail; color composite available
79–91	044° 30'S. 170° 25'E.	21111–21041	06 Feb 78	34	●	0	Good detail in both névé and glacier trunk area
79–91	044° 30'S. 170° 25'E.	30324–21342–A	23 Jan 79	42	◑	20	Landsat 3 RBV; best image for glacier trunk definition; lacks detail in snow
79–91	044° 30'S. 170° 25'E.	30324–21342–C	23 Jan 79	42	●	0	Landsat 3 RBV; best image for glacier trunk definition; lacks detail in snow
80–90	043° 05'S. 169° 32'E.				◕		
80–91	044° 30'S. 168° 59'E.	2824–21211	25 Apr 77	16	◑	30	Marginal; some clouds; definition lost due to low Sun angle contrast
80–91	044° 30'S. 168° 59'E.	30739–21342	13 Mar 80	29	◑	50	Marginal; some clouds; some data lines missing
81–91	044° 30'S. 168° 00'E.	1505–21540	10 Dec 73	49	◑	30	Excellent; some cloud and seasonal snow cover
81–91	044° 30'S. 168° 00'E.	30776–21383	19 Apr 80	19	●	0	Excellent over glacier area; data lines missing on west

Figure 9.—*Oblique aerial photograph looking east on 11 April 1978 at a small unnamed glacier under Mount Kensington (2,446 m) west of the main divide in the Mount Whitcombe region. The glacier, typical of steep Westland glaciers having a high activity index, reacts strongly to climatic changes. Photograph by Trevor J.H. Chinn, New Zealand Geological Survey, film negative no. 7826.*

Figure 10.—*Oblique aerial photograph looking east on 16 April 1980 at the Jalf Glacier, a "dying" glacier on the West Coast between Franz Josef and Fox Glaciers. The surface of bare ice indicates that the snowline has risen completely above the glacier, and no snow at all from recent winters has remained to contribute to the glacier balance. Photograph by Trevor J.H. Chinn, New Zealand Geological Survey, film negative no. 8094.*

Types of Glaciers and Phenomena Observable on Landsat Images

Glacier Advance and Recession

All of New Zealand's glaciers have generally been receding since the beginning of the century (fig. 6), with fluctuating, but rising, end-of-summer snowline elevations. During the "Late Neoglacial" cool period, which persisted during the past 500 to 800 years, most New Zealand glaciers reached three main maximums, climaxing in 1750, 1850, and 1890 (Wardle, 1973; Burrows, 1975; Burrows and Maunder, 1975; Burrows and Russell, 1975; Salinger, 1976; Hessell, 1980, 1983; Salinger and others, 1983). From 1890 there was a general slow recession of most glaciers until the late 1920's, when a widespread rapid retreat commenced. This retreat is continuing, punctuated by only minor readvances in the more active glaciers (fig. 6). Associated with the retreat of glacier termini, most glaciers have suffered a reduction in size and a rise of snowline elevations. From 1971 to 1975, Ivory Glacier lost more than 30 m of thickness in the terminus area, less over other parts of the glacier (fig. 7). The total volume of ice and snow lost during this period for this glacier alone was 13.9×10^6 m^3, or an average annual loss of 3.5×10^6 m^3. During the same period the area of this glacier was reduced by 26 percent, from 0.80 km^2 to 0.59 km^2. Where the larger glaciers extend to low-gradient or ponded ice trunks at valley floor level, recession is evident by a steady lowering of ice-surface levels, accompanied by little or no change in terminus position, or by the development of a proglacial lake. These glaciers have glacier snouts that are normally debris covered, and many have recently developed glacierkarst features. The glacierkarst terrain on Tasman Glacier is well displayed on Landsat 3 RBV image 30324–21342, subscene A (fig. 11). Recently formed proglacial lakes of Classen and Godley Glaciers also appear clearly near the northern margin of this image. Figure 12 is an oblique aerial photograph of Douglas Glacier's proglacial lake, which has developed during the past 20 years. The change in size of proglacial lakes is possibly the single best indicator of glacier variations seen on satellite imagery.

In contrast to the slow response of glaciers with large low-gradient trunks, large glaciers with steep trunks have been very reactive to small mass-balance changes, and the long period of glacier recession during the 20th century has been manifested in a series of small advances superimposed upon a general recession, similar to waves on the seashore at ebbing tide. Franz Josef and Fox Glaciers are of this type (figs. 13 and 14), but unfortunately no usable Landsat images of these glaciers exist. Both glaciers lie in the corners of the available Landsat images and are either poorly displayed or obscured by cloud cover.

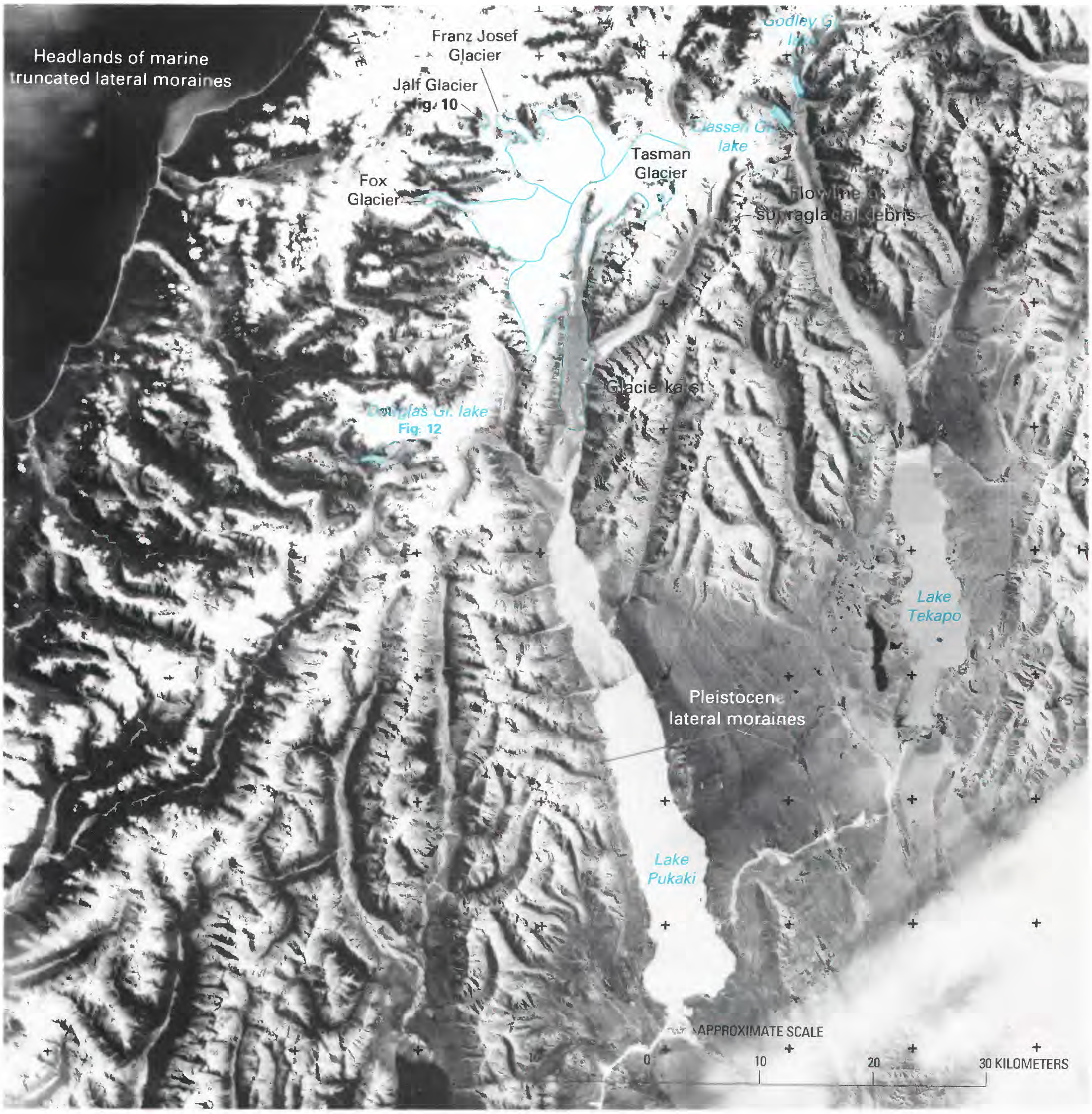

Figure 11.—*Landsat 3 RBV image (30324–21342, subscene A; 23 January 1979; Path 79, Row 91) of part of the Mount Cook region showing glacierkarst features developing on the Tasman Glacier and a wide array of additional glacial features.*

***Figure 12.**—Oblique aerial photograph looking northeast on 11 April 1978 of the debris-covered and detached trunk of Douglas Glacier, which terminates in a rapidly expanding proglacial lake. Photograph by Trevor J.H. Chinn, New Zealand Geological Survey, film negative no. 7830.*

***Figure 13.**—Historic variations of the terminus position of the Franz Josef Glacier and associated events. 1907—A viewing gallery giving access across a sheer rock face above the northeast margin on the snout was scraped off the rock face by this small advance shortly after being built. 1930–1949—A proglacial lake formed but soon filled with outwash gravels. The lake was popular for boating until a large ice block, held submerged by debris, released its load and erupted through the lake surface. 1965—During a heavy rainstorm in December, the main subglacial channel was apparently blocked beneath the glacier snout, and the accumulated water burst upward through the glacier to continue downvalley as a spectacular flood wave of water and ice. There was some damage but no casualties. 1984—A shelter hut, built in 1981 for visitors helicoptered to the inaccessible southwest edge of the glacier snout, was knocked off of its foundation by a large ice block that fell from the glacier front, which was advancing at the rate of a meter per day. The hut was removed from the site, which now remains well under the glacier.* ▷

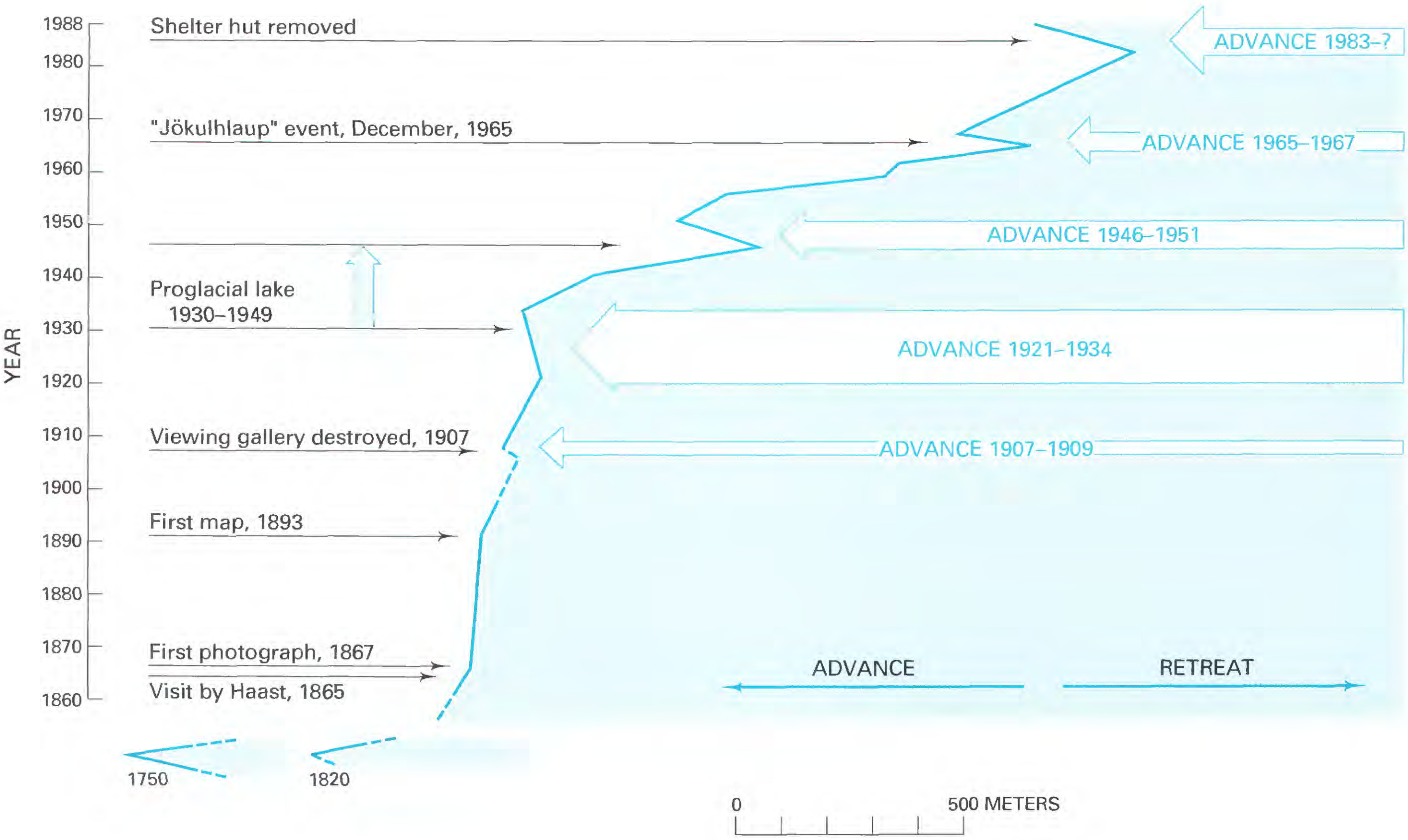

Figure 14.*—Vertical aerial photographic mosaic of the terminus and environs of the Franz Josef Glacier in 1983 showing outlines of positions of the glacier front over the past two centuries. The forest trimline of 1820 is particularly evident. Photograph by P. Mosley, Department of Scientific and Industrial Research, Division of Water Sciences, Wellington.*

Small glaciers have a short-response time to climatic changes (Chinn, 1975). A comparative study of photographs taken during the past 10 years indicates that they may have recently slowed their retreat. Some appear to have even reached a steady state. Unfortunately, the fluctuations of small glaciers cannot be measured or monitored, because the spatial resolution of Landsat MSS and RBV imagery (79-m and 30-m picture elements, or pixels, respectively) is not adequate.

Past glacial extents in both the Pleistocene and Holocene are frequently well depicted on Landsat images. The classic Pleistocene morainal sequences surrounding Lakes Pukaki and Tekapo are well displayed on Landsat MSS image 2805–21163 (fig. 15); the outermost tills are cut by a large canal for a hydroelectric power project. Many of the moraines associated with tributary cirque and valley glaciers also are clearly portrayed. Possibly the largest Pleistocene lateral moraine preserved in New Zealand occurs in south Westland, to the west of the alpine fault. This moraine is shown clearly in the upper lefthand part of Landsat MSS image 2824–21211, band 7 (fig. 16). The successive morainal crests have been progressively moved northeastward by fault displacement, away from the central flowline of the glacier.

Figure 15.—*Landsat 2 MSS false-color composite image (2805–21163; 6 April 1977; Path 79, Row 91) showing Pleistocene glacial features and moraines around Lakes Pukaki, Tekapo, and Ohau.*

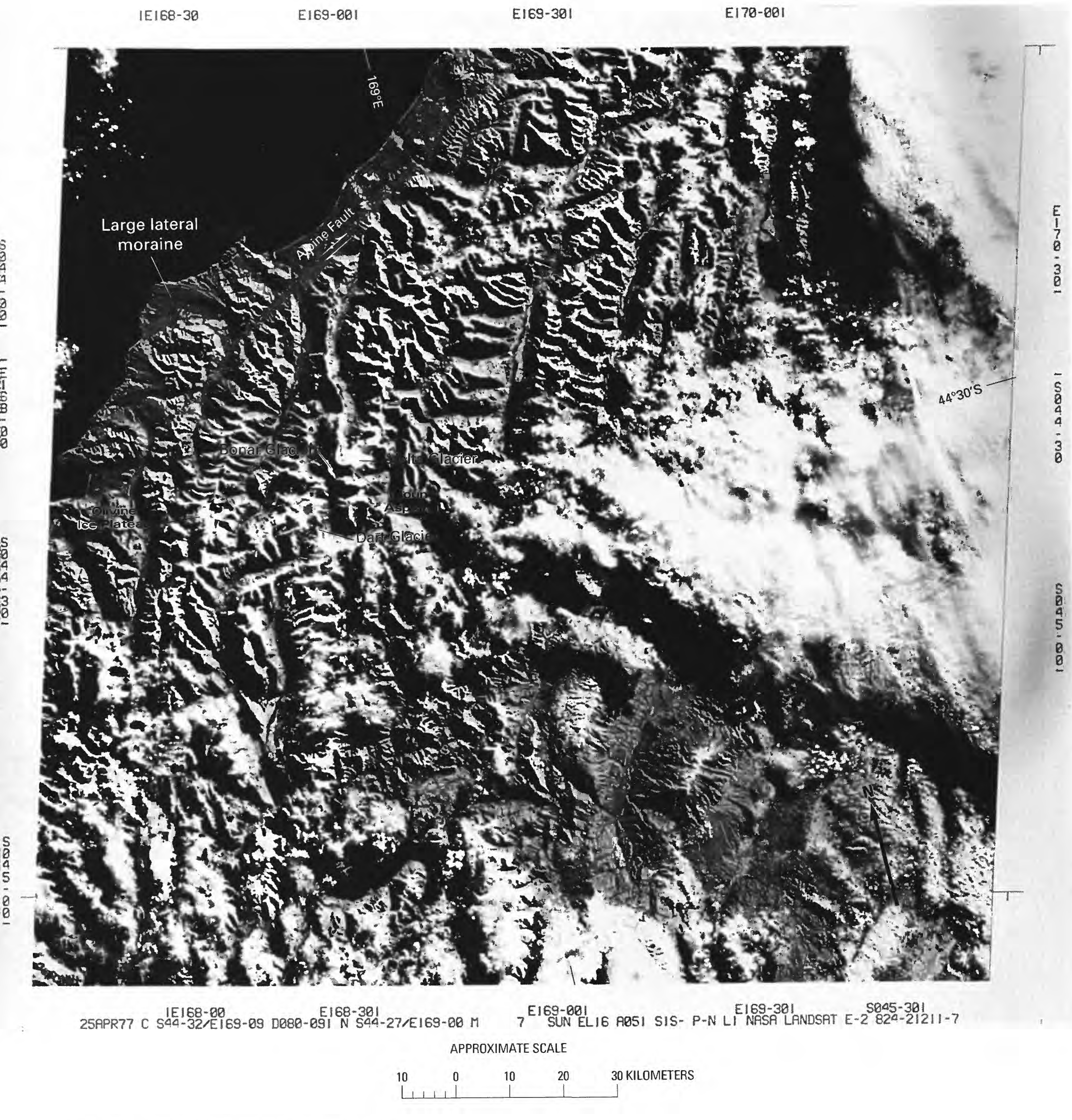

Figure 16.—*Landsat 2 MSS image (2824-21211, band 7; 25 April 1977; Path 80, Row 91) of a large Pleistocene lateral moraine (arrowed). Northward offset by movement along the Alpine fault may be part of the reason for the unusual width of the feature.*

Glacier Flow

Although difficult to see on small glaciers, flow directions can be interpreted on images of the larger glaciers from the patterns of supraglacial morainal debris (fig. 11). Debris-covered glaciers also show flow structures, particularly arcuate structures, in areas of compressive flow. Much of this supraglacial material is derived from rockfalls and landslides, and many of the larger glaciers on the images were found by aerial or field observation to be transporting individual landslides. These features consist of isolated arcuate masses of rock distributed transversely across the glacier trunk (fig. 17). The rate of glacier flow may be estimated from these features by measuring displacement between images made some years apart.

Climatic Variations

The elevation of the end-of-summer snowline on a glacier depends on winter snowfall and summer melt, and changes in snowline position from year to year reflect the precipitation and temperature regimes for the previous year. Snowline positions may be delineated on the larger glaciers, particularly where there is little relief and the glacier gradient is low. The demarcation between snow and bare ice shows up as the boundary between blues and whites on Landsat MSS color-composite images, or as differences in gray tone on black-and-white images (individual Landsat MSS bands 4, 5, 6, or 7).

Variations in glacier-snowline position are probably the single best indicator of a glacier's health. This line separates the accumulation area from the ablation area, and a rise in snowline elevation above its mean

Figure 17.—*Oblique aerial photograph on 14 March 1980 of a recent rock avalanche that fell onto Murchison Glacier during December 1979. Such deposits are readily visible on satellite images. Their movement and distortion enable ice movement to be monitored by satellite imagery. Photograph by Trevor J. H. Chinn, New Zealand Geological Survey, film negative no. 8025.*

position indicates a negative glacier balance. Continued annual negative balances ultimately result in glacier recession. Glacier-snowline elevations have been recorded during studies on the Tasman and Ivory Glaciers (Chinn and Bellamy, 1970; Anderton and Chinn, 1978; Anderton, 1975) and are compared in table 2. During the studies on the Ivory Glacier, the end-of-season snowlines rose above the upper elevation limit of the glacier to an indeterminate elevation on the headwall. Therefore, mass-balance figures are given instead of snowline elevation.

TABLE 2.—*Glacier-snowline variations with time*

Balance year	Tasman Glacier, snowline elevation (m)	Ivory Glacier, area averaged mass balance (m)
1966	1,700	
1967	1,970	
1968	1,630	
1969	1,690	
1970	2,200	−2.11[1]
1971	1,930	−1.66[1]
1972	1,850	−1.73
1973	1,900	−3.48
1974	1,700	−4.00
1975	1,680	
1976	1,680	
1977	1,770	
1978	1,860	
1979	1,700	
1980	1,810	
1981	1,750	
1982	1,750	
1983	1,740	
1984	1,720	
1985	1,720	
Mean	1,790	

[1] Approximately one full year only.

Conclusions

Glaciers are particularly useful for the study of present and past climatic variations. A record of variations in glacier margins and glacier-snowline positions provides a means of accurately documenting yearly climatic variations, whereas moraines mark previous glacier extents and thus record past colder climates. Satellite imagery is a fast and regionally comprehensive method of documenting all of these glacier features. In New Zealand, satellite imagery may have its greatest value in establishing past limits of the larger glaciers, because former moraines and other subtle ground features clearly show former glacier extent. The limiting factor of Landsat images of New Zealand for glaciological monitoring is the effective spatial resolution of MSS, Landsat 3 RBV, and thematic mapper (TM) data (79-m pixels for the MSS, 30-m pixels for the RBV and TM images). Future satellite images, such as photographs from the Large Format Camera, which have a spatial resolution of 10 m (equivalent to a 3-m pixel), will result in a major reassessment of the value of satellite imagery for monitoring fluctuations in New Zealand's glaciers.

References Cited

Anderton, P.W., 1973, The significance of perennial snow and ice to the water resources of the South Island, New Zealand: Journal of Hydrology (New Zealand), v. 12, no. 1, p. 6–18.

———compiler, 1975, Tasman Glacier 1971-73: Wellington, Ministry of Works and Development for the National Water and Soil Conservation Organization, Hydrological Research, Annual Report No. 33, 28 p.

Anderton, P.W., and Chinn, T.J., 1978, Ivory Glacier, New Zealand, and I.H.D. representative basin study: Journal of Glaciology, v. 20, no. 82, p. 67–84.

Andrews, J.T., and Miller, G.H., 1972, Quaternary history of the northern Cumberland Peninsula, Baffin Island, N.W.T., Canada: Part IV: Maps of the present glaciation limits and lowest equilibrium line altitude for north and south Baffin Island: Arctic and Alpine Research, v. 4, no. 1, p. 45–59.

Bell, J.M., 1910, A geographical report on the Franz Josef Glacier, with topographical maps and data by R.P. Grenville and botanical notes by Leonard Cockayne: New Zealand Geological Survey, Wellington, 14 p.

Bowen, F.E., 1960, Advances and retreats of the Franz Josef Glacier: Journal of Glaciology, v. 3, no. 28, p. 742.

Burrows, C.J., 1975, Late Pleistocene and Holocene moraines of the Cameron Valley, Arrowsmith Range, Canterbury, New Zealand: Arctic and Alpine Research, v. 7, no. 2, p. 125–140.

Burrows, C.J., and Maunder, B.R., 1975, The recent moraines of the Lyell and Ramsay Glaciers, Rakaia Valley, Canterbury: Journal of the Royal Society of New Zealand, v. 5, no. 4, p. 479–491.

Burrows, C.J., and Russell, J.B., 1975, Moraines of the Upper Rakaia Valley: Journal of the Royal Society of New Zealand, v. 5, no. 4, p. 463–477.

Chinn, T.J., 1969, Snow survey techniques in the Waitaki Catchment, South Canterbury: Journal of Hydrology (New Zealand), v. 8, no. 2, p. 68–76.

———1975, Late Quaternary snowlines and cirque moraines within the Waimakariri watershed: M.Sc. thesis, University of Canterbury, New Zealand, 213 p.

———1979, How wet is the wettest of the wet west coast?: New Zealand Alpine Journal, v. 32, p. 85–87.

Chinn, T.J., and Bellamy, R.J., 1970, Ivory Glacier, representative basin for the glacial hydrological region: Wellington, Ministry of Works and Development for the National Water and Soil Conservation Organization, Hydrological Research, Annual Report No. 1, 12 p.

Chinn, T.J., and Whitehouse, I.E., 1980, Glacier snow line variations in the Southern Alps, New Zealand, *in* World Glacier Inventory, Riederalp (Switzerland) Workshop, Proceedings: International Association of Hydrological Sciences, IAHS–AISH Publication No. 126, p. 219–228.

Ferrigno, J.G., and Williams, R.S., Jr., 1983, Limitations is the use of Landsat images for mapping and other purposes in snow- and ice-covered regions: Antarctica, Iceland, and Cape Cod, Massachusetts, *in* Proceedings of the Seventeenth International Symposium on Remote Sensing of Environment: Environmental Research Institute of Michigan, Ann Arbor, Michigan, v. 1, p. 335–355.

FitzGerald, E.A., 1896, Climbs in the New Zealand Alps: London, Fisher Unwin, 363 p.

Gellatly, A.F., 1985, Historical records of glacier fluctuations in Mt. Cook National Park, New Zealand: A century of change: The Geographical Journal, v. 151, no. 1, p. 86–99.

Goldthwaite, R.P., and McKellar, I.C., 1962, New Zealand glaciology, *in* Wexler, H., and others, eds., Antarctic Research: American Geophysical Union, Geophysical Monograph 7, p. 209–216.

Griffiths, G.A., and McSaveney, M.J., 1983, Distribution of mean annual precipitation across some steepland regions of New Zealand: New Zealand Journal of Science, v. 26, no. 2, p. 197–209.

Gunn, B.M., 1964, Flow rates and secondary structures of Fox and Franz Josef Glaciers, New Zealand: Journal of Glaciology, v. 5, no. 38, p. 173–190.

Harper, A.P., 1896, Pioneer work in the Alps of New Zealand; a record of the first exploration of the chief glaciers and ranges of the Southern Alps: London, T.F. Unwin, 336 p.

———1946, Memories of mountains and men: Christchurch, Simpson and Williams, Ltd., 208 p.

Heine, A.J., 1962, Glacier changes on Mount Ruapehu, New Zealand, 1957-1961, *in* Symposium of Obergurgl (Austria), Variations of the regime of existing glaciers: International Association of Scientific Hydrology Publication No. 58, p. 173–178.

Hessell, J.W.D., 1980, Apparent trends of mean temperature in New Zealand since 1930: New Zealand Journal of Science, v. 23, no. 1, p. 1–9.

———1983, Climatic effects on the recession of the Franz Josef Glacier: New Zealand Journal of Science, v. 26, no. 3, p. 315–320.

Krenek, L.O., 1959, Changes in the glaciers of Mount Ruapehu: New Zealand Journal of Geology and Geophysics, v. 2, no. 4, p. 643–653.

Mannering, G.E., 1891, With axe and rope in the New Zealand Alps: London, Longman, Green and Co., 139 p.

McSaveney, M.J., and Gage, M., 1968, Ice flow measurements on Franz Josef Glacier, New Zealand, in 1966: New Zealand Journal of Geology and Geophysics, v. 11, no. 3, p. 564–592.

Mercer, J.H., 1967, Glaciers of New Zealand, *in* Southern hemisphere glacier atlas: Technical Report 67–76–ES by the American Geographical Society, New York, for the Earth Sciences Laboratory, U.S. Army Natick Laboratories, Natick, Massachusetts, Series ES–33, June, p. 209–239.

Odell, N.E., 1955, Mount Ruapehu, New Zealand: Observations on its crater lake and glaciers: Journal of Glaciology, v. 2, no. 18, p. 601–605.

Pascoe, J.D., ed., 1957, Mr. Explorer Douglas: Wellington, A.H. and A.W. Reed, 331 p.

Porter, S.C., 1975, Glaciation limit in New Zealand's Southern Alps: Arctic and Alpine Research, v. 7, no. 1, p. 33–37.

Salinger, M.J., 1976, New Zealand temperatures since 1300 AD: Nature, v. 260, no. 5549, p. 310–311.

Salinger, M.J., Heine, M.J., and Burrows, C.J., 1983, Variations of the Stocking (Te Wae Wae) Glacier, Mount Cook, and climatic relationships: New Zealand Journal of Science, v. 26, no. 3, p. 321–338.

Sara, W.A., 1968, Franz Josef and Fox Glaciers, 1951–67: New Zealand Journal of Geology and Geophysics, v. 11, no. 3, p. 768–780.

———1970, Glaciers of Westland National Park: Wellington, New Zealand Department of Scientific and Industrial Research, Information Series No. 75, 46 p.

Skinner, B.E., 1964, Measurement of twentieth century ice loss on the Tasman Glacier, New Zealand: New Zealand Journal of Geology and Geophysics, v. 7, no. 4, p. 796–803.

Soons, J.M., 1971, Recent changes in the Franz Josef Glacier, *in* Johnston, R.J., and Soons, J.M., eds., Proceedings of the Sixth New Zealand Geography Conference, Christchurch, August 1970: New Zealand Geographical Society, Conference Series No. 6, v. 1, p. 195–200.

Speight, R., 1939, Some aspects of glaciation in New Zealand: Report of the Australian and New Zealand Association for the Advancement of Science, v. 24, p. 49–71.

Suggate, R.P., 1950, Franz Josef and other glaciers of the Southern Alps, New Zealand: Journal of Glaciology, v. 1, no. 8, p. 422–429.

Thompson, R.D., and Kells, B.R., 1973, Mass balance studies on the Whakapapanui Glacier, New Zealand, *in* The role of snow and ice in hydrology, Banff Symposium (1972), Proceedings: International Association of Hydrological Sciences, IAHS–AISH Publication No. 107, v. 1, no. 1 (Symposium on Properties and Processes (UNESCO)), p. 383–393.

Wardle, P., 1973, Variations of the glaciers of Westland National Park and the Hooker Range, New Zealand: New Zealand Journal of Botany, v. 11, p. 349–388.